



Sveučilište u Zagrebu
PRIRODOSLOVNO-MATEMATIČKI FAKULTET
Kemijski odsjek

Petra Vizjak

MAPIRANJE POVRŠINSKI IZLOŽENIH CISTEINA U ATP-azi ISWI

Diplomski rad

predložen Kemijskom odsjeku
Prirodoslovno-matematičkog fakulteta Sveučilišta u Zagrebu
radi stjecanja akademskog zvanja
magistre kemije

Zagreb, 2017.

Ovaj diplomski rad izrađen je u Biomedicinskom centru Sveučilišta Ludwig Maximilian u Münchenu pod mentorstvom i neposrednim voditeljstvom dr. Felixa Müllera-Planitza.
Nastavnik imenovan od strane Kemijskog odsjeka je doc. dr. sc. Marko Močibob

Gratitudes

I want to thank to dr. Felix Müller Planitz for giving me the opportunity to do this Master thesis and to dr. Andreas Schmidt for the help with mass spectrometry analysis.

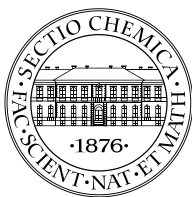
Želim zahvaliti kolegama, prijateljima i obitelji koji su mi pomagali tijekom studija.

Također želim zahvaliti prof. dr. sc. Snežani Miljanić za pomoć u završavanju ovog studija i doc. dr. sc. Marku Močibobu na kritičkom čitanju ovog rada.

Table of Contents

SAŽETAK.....	IX
ABSTRACT	XI
§ 1. INTRODUCTION	1
1.1. The aim.....	2
§ 2. LITERATURE REVIEW	3
2.1. Chromatin.....	3
2.2. Chromatin remodeling complexes	4
2.2.1. <i>The SWI/SNF family.....</i>	<i>5</i>
2.2.2. <i>The CHD family.....</i>	<i>5</i>
2.2.3. <i>The INO80 family.....</i>	<i>6</i>
2.2.4. <i>The ISWI family.....</i>	<i>6</i>
2.3. ATPase ISWI.....	7
2.4. Thiol-reactive probes	8
2.4.1. <i>Reactivity of thiol groups</i>	<i>9</i>
2.4.2. <i>Iodoacetic acid.....</i>	<i>10</i>
2.4.3. <i>Maleimides.....</i>	<i>10</i>
2.4.4. <i>Ellman's reagent</i>	<i>11</i>
2.4.5. <i>2-nitro-5-thiocyanobenzoic acid (NTCB)</i>	<i>11</i>
2.5. Mapping protein structure changes with cysteine labeling.....	13
§ 3. MATERIALS AND METHODS	14
3.1. Materials	14
3.1.1. <i>Chemicals.....</i>	<i>14</i>
3.1.2. <i>Enzymes.....</i>	<i>14</i>
3.1.3. <i>Stock solutions.....</i>	<i>14</i>
3.1.4. <i>Buffers.....</i>	<i>14</i>
3.1.5. <i>E. coli strains</i>	<i>15</i>
3.2. Methods.....	15
3.2.1. <i>Recombinant overexpression and purification of ATPase ISWI.....</i>	<i>15</i>
3.2.2. <i>Removal of DTT.....</i>	<i>19</i>
3.2.3. <i>Assays with Ellman reagent</i>	<i>19</i>
3.2.4. <i>Reaction with NTCB.....</i>	<i>19</i>
3.2.5. <i>Reaction with alkylating reagents.....</i>	<i>19</i>

§ Table of Contents	vii
3.2.6. <i>Mass spectrometry</i>	20
3.2.7. <i>Cysteine mapping in bacterial lysate</i>	20
§ 4. RESULTS AND DISCUSSION	23
4.1. Cysteine mapping in purified ATPase ISWI	23
4.1.1. <i>Purification of ATPase ISWI</i>	23
4.1.2. <i>Determination of the molar extinction coefficient of 2-nitro-5-thiobenzonate dianion</i>	28
4.1.3. <i>Adapting the assay for the smaller quantities the of analyte</i>	31
4.1.4. <i>Reaction of the ATPase ISWI with Ellman reagent</i>	35
4.1.6. <i>Reaction of ISWI with iodoacetic acid and N-ethylmaleimide</i>	37
4.2. Cysteine mapping in bacterial lysate	39
§ 5. CONCLUSION	43
§ 6. ABBREVIATIONS	45
§ 7. LITERATURE	46
§ 8. CURRICULUM VITAE	XVI



Sveučilište u Zagrebu
Prirodoslovno-matematički fakultet
Kemijski odsjek

Diplomski rad

SAŽETAK

MAPIRANJE POVRŠINSKI IZLOŽENIH CISTEINA U ATP-azi ISWI

Petra Vizjak

U eukariotskoj stanici, molekula DNA nalazi se u obliku kromatina. Ponavljajuća jedinica kromatina je nukleosom, 147 parova baza DNA namotano oko histonskog oktamera. Položaj nukleosoma na DNA ima važnu ulogu u kontroli transkripcije. Remodelirajući protein ISWI (*Drosophila melanogaster*) pomiče nukleosome duž DNA. Cilj ovog rada je mapirati površinski izložene cisteine proteina ISWI. Rezultati će kasnije biti iskorišteni za analizu postojećih strukturnih modela proteina ISWI. Cisteini koji se nalaze na površini proteina, brže podliježu kemijskim reakcijama. Kako bi se potvrdilo da cisteini reagiraju različitom kinetikom, korišteni su reagensi za spektrofotometrijsko utvrđivanje tiola: 5,5'-ditiobis-(2-nitrobenzojeva kiselina) i 2-nitro-5-tiocianatobenzojeva kiselina. Za točnu identifikaciju površinski izloženih cisteina, ISWI je tretiran s primarnim alkilirajućim reagensom (*N*-etilmaleimidom), denaturiran i tretiran sa sekundarnim alkilirajućim reagensom (jodoctenom kiselinom). Produkt tih dviju reakcija je dodatak različitih modifikacijskih skupina na cisteine, koje se potom mogu razlučiti spektrometrijom masa. Polovica od ukupnih cisteina mogla se klasificirati kao površinski izloženi ili zaklonjeni unutar strukture proteina.

(48 stranica, 30 slika, 10 tablica, 59 literaturnih navoda, jezik izvornika: engleski)

Rad je pohranjen u Središnjoj kemijskoj knjižnici Prirodoslovno-matematičkog fakulteta Sveučilišta u Zagrebu, Horvatovac 102a, Zagreb i Repozitoriju Prirodoslovno-matematičkog fakulteta Sveučilišta u Zagrebu

Ključne riječi: alkiliranje cisteina, Ellman, ISWI, mapiranje cisteina, NTCB

Mentor: dr. sc. Felix Müller-Planitz, voditelj grupe

Nastavnik (imenovan od strane Kemijskog odsjeka): doc. dr. sc. Marko Močibob

Ocjenitelji:

1. doc. dr. sc. Marko Močibob
2. izv. prof. dr. sc. Branimir Bertoša
3. doc. dr. sc. Đani Škalamera

Zamjena: doc. dr. sc. Jasmina Rokov Plavec

Datum diplomskog ispita: 29. rujna 2017.



University of Zagreb
Faculty of Science
Department of Chemistry

Diploma Thesis

ABSTRACT

MAPPING OF SURFACE-EXPOSED CYSTEINES IN ATPase ISWI

Petra Vizjak

In an eukaryotic cell, DNA molecule exists in the form of chromatin. The repetitive unit of chromatin is a nucleosome, 147 bp of DNA wrapped around histone octamer. Nucleosome position along DNA is important for transcription regulation. Chromatin remodeler ISWI (*Drosophila melanogaster*) slides nucleosomes along DNA. The aim of this work is to map surface-exposed cysteines in the protein ISWI. The surface-exposed cysteines are easily available for chemical reaction. To probe accessibility of cysteines for chemical reaction, commonly used reagents for spectrophotometric detection of thiols were used: 5,5'-dithiobis-(2-nitrobenzoic acid) and 2-nitro-5-thiocyanatobenzoic acid. To unequivocally identify surface-exposed cysteines, ISWI was treated with primary alkylating reagent (*N*-ethylmaleimide), denatured and treated with secondary alkylating reagent (iodoacetic acid). The two reactions add to the cysteine different modification groups which can be discriminated by mass spectrometry. Half of the total cysteines could be classified either as buried or surface-exposed in the protein structure.

(48 pages, 30 figures, 10 tables, 59 references, original in english)

Thesis deposited in Central Chemical Library, Faculty of Science, University of Zagreb, Horvatovac 102a, Zagreb, Croatia and in Repository of the Faculty of Science, University of Zagreb

Keywords: cysteine mapping, cysteine alkylation, Ellman, ISWI, NTCB

Mentor: dr. sc. Felix Müller-Planitz, group leader
Supervisor: doc. dr. sc. Marko Močibob

Reviewers:

1. doc. dr. sc. Marko Močibob
2. izv. prof. dr. sc. Branimir Bertoša
3. doc. dr. sc. Đani Škalamera

Substitute: doc. dr. sc. Jasmina Rokov Plavec

Date of exam: September 29th, 2017

§ 1. INTRODUCTION

In an eukaryotic cell, long DNA must be condensed and accessed in coordinated fashion to allow for proper transcription, replication, recombination, repair and other chromosomal processes. To accomplish this task, DNA molecule exists in the form of chromatin, dynamic polymeric complex. The repetitive unit of chromatin is a nucleosome core particle, 147 bp of DNA wrapped around histone octamer. Histone octamer contains two copies of each of core histones: H2A, H2B, H3 and H4. Neighbouring nucleosome core particles are connected with a short linker DNA. Linker DNA and nucleosome core particle together build a nucleosome. Nucleosome position along DNA strand is important for transcription regulation and chromatin folding. ATP-dependent nucleosome remodeling complexes (remodelers) can move, eject and restructure nucleosomes thereby ensuring proper density and spacing of nucleosomes. Chromatin remodeler ISWI slides nucleosomes along DNA.

There is a very limited structural information on the remodelers. It appears that a remodeler undergoes a large conformational change upon engagement with the substrate. Even less is known about the precise mechanism of the remodelling reaction and about intrinsic structural changes in the remodeler. For the ATPase ISWI (*D. melanogaster*), a few models have been derived from the crosslinking experiments as well as from the cryo electron microscopy and the crystallographic studies of the related proteins. Our lab recently applied the integrative structural biology approach to probe the ISWI structure in solution. The obtained model predicts that the C-terminal HAND-SAND-SLIDE (HSS) module packs against the ATPase domain through its SLIDE domain. To verify the model, we decided to assess the change in cysteines accessibility upon deletion of HSS domain. The change in the exposure (or the lack of) of the particular cysteines, will help us to judge the validity of the derived model.

1.1. The aim

To test the current model of ISWI structure in solution, we wanted to make use of many cysteine residues present in the primary structure of the ATPase ISWI. The protein has 11 cysteines, whose exposure on the surface might be different in the different protein conformations. Different surface exposure would affect the rate of their reactions with thiol-reactive reagents. The aim of this work is to map surface exposed cysteines in the ATPase ISWI.

The obtained knowledge will later be used to verify suggested conformational changes upon substrate binding and in an active state.

§ 2. LITERATURE REVIEW

2.1. Chromatin

In a human cell, 2 meters long DNA molecule must be organized within a nucleus with an average diameter of 5-10 μm .¹ At the same time, DNA has to be continuously accessed in a coordinated fashion to allow for proper transcription, repair, replication and recombination. To accomplish this task, the genome is organized in a dynamic polymeric complex – chromatin. The repeating unit of chromatin is a nucleosome core particle, 147 base pairs (bp) of DNA wrapped around histone octamere. Histone octamere consists of two copies of each of core histones: H2A, H2B, H3 and H4 (Fig. 1).

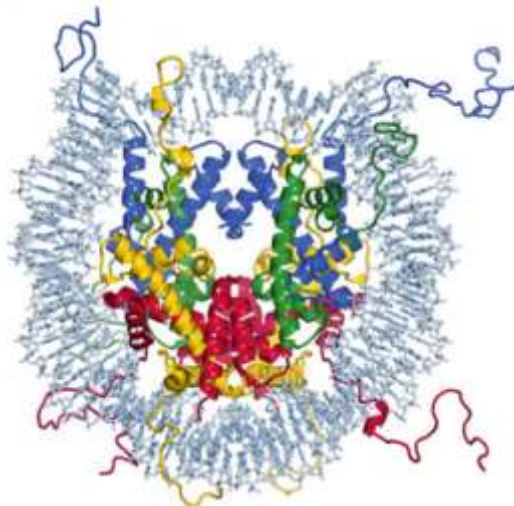


Figure 1. Overview of the nucleosome core particle structure. Nucleosome core particle high resolution structure (PDB ID: 1KX5). Histones are depicted in cartoon representation and coloured as shown. DNA is depicted in stick representation. H2A (yellow), H2B (red), H3 (blue), H4 (green).²

Two nucleosomes core particles are separated with a stretch of linker DNA. The length of linker DNA ranges from 20 to 90 bp.³ Linker DNA can sometimes be bound with the linker histone. Nucleosome core particle and linker DNA together form a nucleosome. Chromatin is composed of long arrays of nucleosomes (Fig. 2), which can condense in higher order structures.

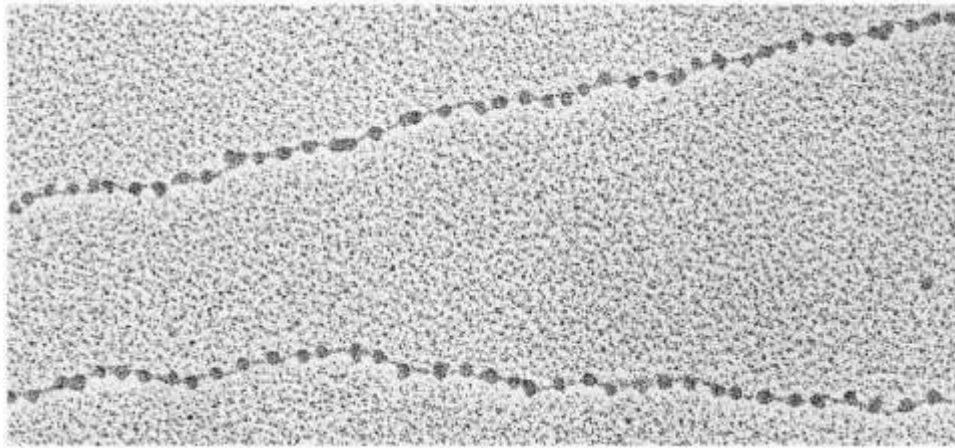


Figure 2. Unfolded chromatin –“beads on a string”(electron micrograph)⁴

2.2. Chromatin remodeling complexes

DNA has to balance two opposing needs at the same time – the need to be condensed and the need to be accessible to the factors that conduct transcription, replication, recombination and repair. These processes involve action of ATP-dependent chromatin remodeling complexes (remodelers) which ensure proper density and spacing of nucleosomes. Remodelers are distinguished from other chromatin factors by their use of the energy of ATP hydrolysis to promote these functions. They can modify chromatin structure by assembling or evicting nucleosomes, changing the composition of the octamer or sliding nucleosomes along the DNA (Fig 3.).

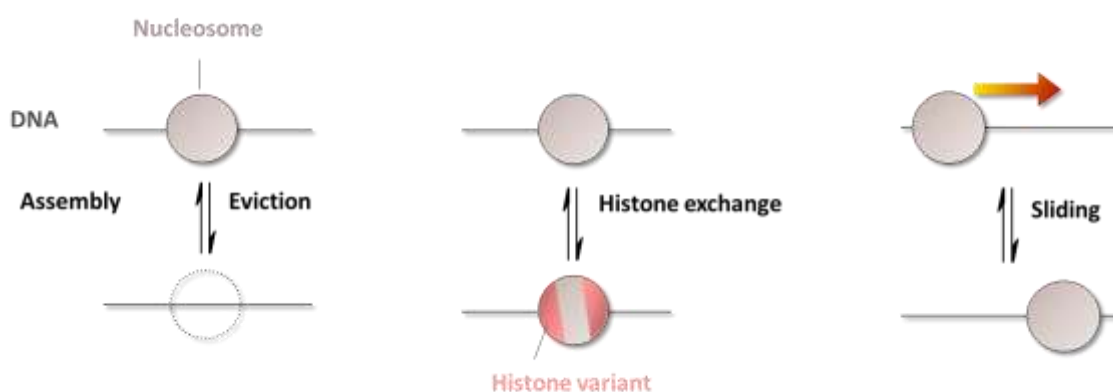


Figure 3. Functions of chromatin remodeling complexes (figure prepared by F. Müller-Planitz).

The catalytic subunit of the remodeling enzyme consists of a conserved ATPase domain which contains two tandem RecA-like folds (DExx and HELICc) (Fig. 4). This enzymes belong to the Superfamily 2 of helicase-like proteins. With respect to different domains that flank the conserved ATPase domain, remodelers are grouped in 4 families: SWI/SNF, CHD, ISWI and INO80.^{5,6}

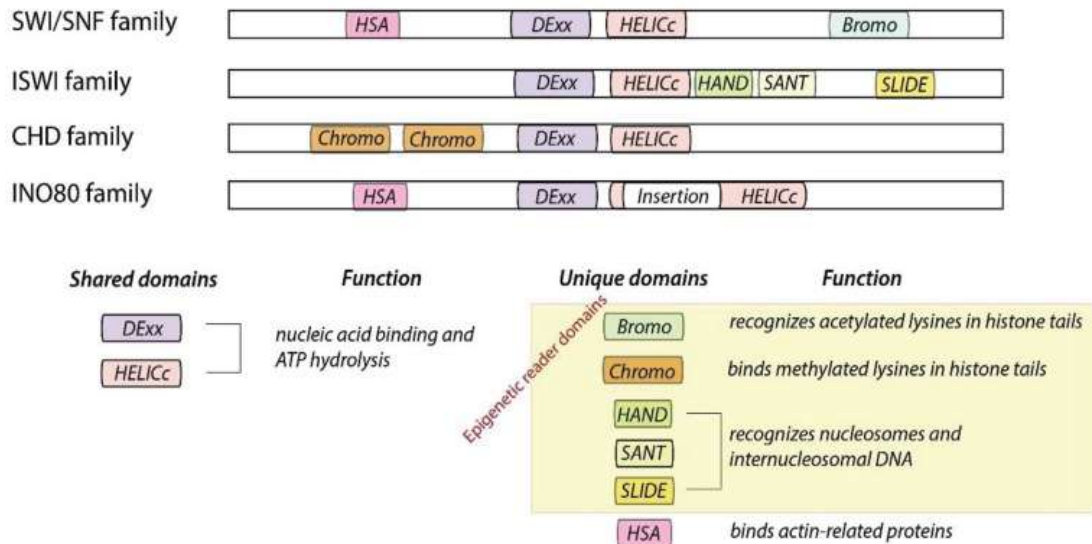


Figure 4. Organization of remodeler families defined by their catalytic and flanking domains. All remodeling enzymes consist of a shared ATPase domain and unique flanking domains.⁷

2.2.1. The SWI/SNF family

The SWI/SNF family members have an N-terminally located HSA (helicase-SANT) domain, which is known to recruit actin and actin-related proteins, and a C-terminally located bromo domain, known to bind to the acetylated lysines of histones.⁸ Members of this family of remodelers are large, multi-subunit complexes containing eight or more proteins. They can slide and evict nucleosomes from DNA. Variant subunits are thought to contribute to targeting, assembly and regulation of lineage-specific functions of those complexes.^{9,10,11}

2.2.2. The CHD family

The CHD family (Chromodomain-Helicase-DNA binding) is defined by the presence of two chromo domains in tandem, at the N-terminal of the ATPase domain. Additional structural motifs are used to further divide the CHD family into the subfamilies CHD1, Mi-2 and CHD7.^{6,12}

Members of the CHD1 subfamily contain a C-terminal DNA-binding domain that preferentially binds to AT-rich DNA *in vitro*.^{13,14} Members are Chd1 and Chd2 in higher eukaryotes. The crystal structure of the DNA binding domain of Chd1, revealed a SANT-SLIDE like fold. This domain is required for the remodeling activity of Chd1 *in vitro* and *in vivo*.¹⁵ The Mi-2 subfamily members contain a pair of PHD domains (plant homeodomain) in their N-terminal part, implicated in nucleosome binding.¹⁶ The CHD7 subfamily members have additional C-terminal domains.

The biological properties of CHD family members are highly heterogeneous. Some exist as monomers *in vivo*; others are subunits of multiprotein complexes, many of which have not yet been fully characterized.¹⁷

2.2.3. The INO80 family

The characteristic of the remodelers belonging to the INO80 family (inositol requiring 80) is the split ATPase domain. This unique module retains ATPase activity, and acts as a scaffold for the association with the RuvB-like proteins, Rvb1 and Rvb2.¹⁹ Unlike remodelers of other families, the INO80 complex exhibits DNA helicase activity and binds to specialized DNA structures *in vitro*.^{20,21} Some of these remodelers exhibit histone-exchange activity^{22,23} and can slide nucleosomes *in vitro* on a reconstituted chromatin template and evict histones from DNA.^{24,25,26}

2.2.4. The ISWI family

The ISWI family (Imitation SWItch) ATPases harbor a C-terminal SANT domain adjacent to a SLIDE domain (SANT-like ISWI), which together form a nucleosome recognition module that binds to DNA and H4 tails.²⁷ The ISWI remodeling enzyme in *D. melanogaster*, is known to be present in several chromatin remodeling complexes such as NURF, CHRAC, ACF and RSF. Snf2H and Snf2L are the mammalian homologues of ISWI, which act in the presence of one to three accessory subunits forming different remodeling complexes with different properties. Many ISWI family complexes (ACF, CHRAC and NoRC) catalyze nucleosome spacing, promote chromatin assembly, compaction of higher order structures of chromatin and are generally involved in transcriptional repression.^{28,29,30}

2.3. ATPase ISWI

The ATPase ISWI (*D. melanogaster*) is the catalytic core of several multiprotein nucleosome remodeling machines.³¹ ISWI mutations affect both cell viability and gene expression during *Drosophila* development.³² ISWI ATPase is an autonomous remodeling machine and it slides nucleosomes along DNA.³³ The domain structure of ISWI is presented in the Figure 5.



Figure 5. The domain structure of ISWI.

The ATPase domain is composed from two distinct lobes. The C-terminal HAND–SAND–SLIDE (HSS) domain functions in binding extranucleosomal linker DNA.^{34,35,36,37} The activity of the catalytic core of ISWI is inhibited by the regulatory AutoN (part of NTR domain) and NegC domains, which are in turn antagonized by the H4 tail and extranucleosomal DNA.³¹ Mechanism of remodeling and its regulation with ATPase flanking domains are still elusive.

Not many structural studies have been performed on ATP-dependent chromatin remodelers. Recently, the crystal structure of ISWI from the *Myceliophthora thermophila* and its complex with a histone H4 peptide has been published. The structure shows the N-terminal AutoN domain binding the lobe 2, thus holding the enzyme in an inactive conformation. The H4 peptide binds to the lobe 2 coincident with one of the AutoN-binding sites, explaining the ISWI activation by H4. The C-terminal NegC domain is involved in binding to the lobe 2 domain and functions as an allosteric element for ISWI to respond to the extranucleosomal DNA length.³⁸

The ISWI structure has also been probed with crosslinks.^{39,40} Our lab recently applied the integrative structural biology approach to probe the ISWI structure in solution. The obtained model predicts that the HSS module packs against the ATPase domain through its SLIDE domain in the ATPase resting state.

2.4. Thiol-reactive probes

Thiol-reactive probes are used to label proteins for the detection of conformational changes, assembly of multisubunit complexes and ligand-binding processes. They primarily react with cysteine residues.

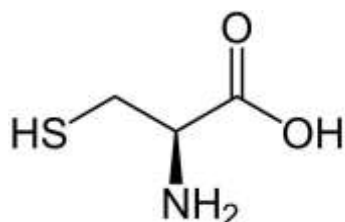


Figure 6. L-Cysteine⁴¹

Thiols have an important role in maintaining the oxidation-reduction state of proteins (Fig 7.). Many reagents and methods have been developed for the quantification of thiols and disulfides.

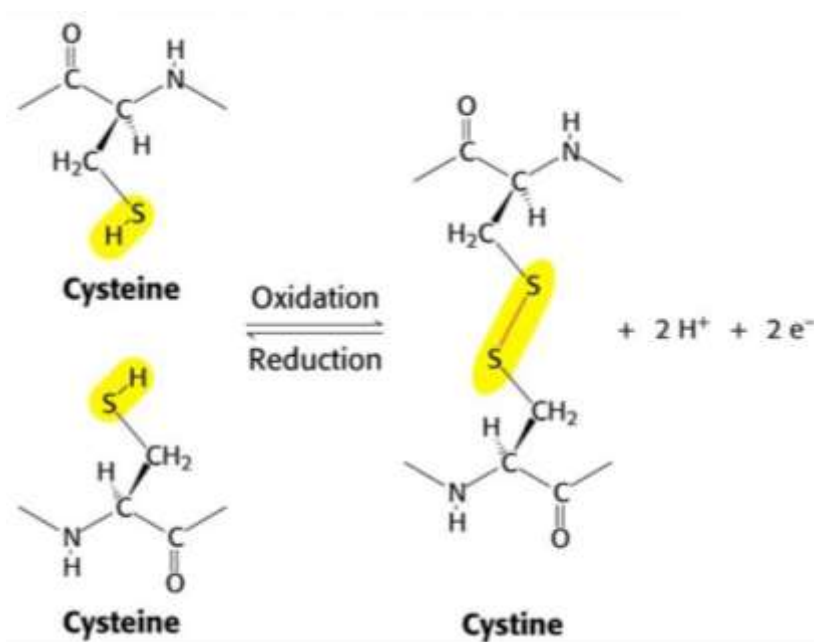


Figure 7. Reversible oxidation of two cysteine residues results in a formation of a disulfide bridge.⁴²

2.4.1. Reactivity of thiol groups

Cystine disulfides can be reduced with dithiothreitol (DTT) or β -mercaptoethanol. These reducing agents have to be removed before reaction with the thiol-reactive probe. Removal of DTT or 2-mercaptoethanol causes oxidation of the thiols back to the disulfides, due to the oxygen dissolved in buffers. This can be avoided by degassing all used buffers under the vacuum. Alternatively, tris-(2-carboxyethyl)phosphine (TCEP) might be used. TCEP is the reducing agent which does not contain thiols, but some researchers reported that it reacts with few commonly used labeling reagents.⁴³

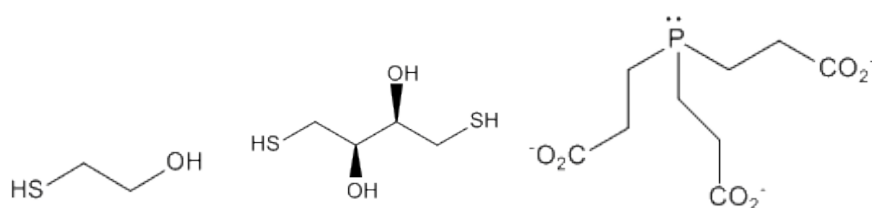


Figure 8. Skeletal formulas of thiol-reducing reagents. From left to right: 2-mercaptoethanol, dithiothreitol and tris-(2-carboxyethyl)phosphine.⁴³

Alkyl halides, haloacetamides and maleimides react by S-alkylation of thiols to generate thioether (Fig. 9 and Fig. 10). Cysteine is more reactive above its pK_a (~8.3, depending on protein structural context) since it is present in the form of the thiolate anion which is a better nucleophile than the neutral thiol.⁴³



Figure 9. Reaction scheme of a thiol with an alkyl halide.⁴³

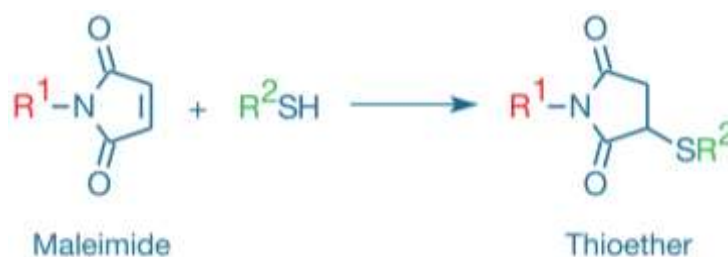


Figure 10. Reaction scheme of a thiol with a maleimide.⁴³

2.4.2. Iodoacetic acid

Iodoacetic acid (IAA) readily reacts with all thiols, including those found in proteins to form thioethers (Fig. 11). The relative reaction rates between glutathione and these halogenated acetates are 100:60:1 for iodo-, bromo- and chloro-acetates, respectively.⁴³

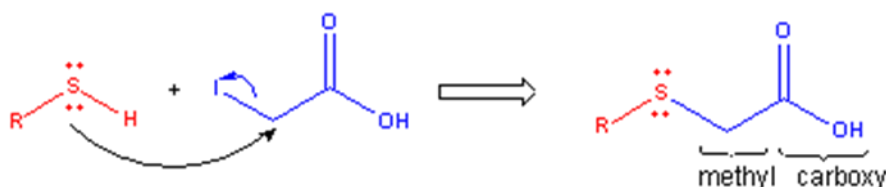


Figure 11. Reaction scheme of iodoacetic acid with cysteine residue in the protein (carboxymethylation by S_N2 mechanism).⁴³

IAA can react with amines, however, most aliphatic amines, except the α -amino group at a protein's N-terminus, are protonated and thus relatively unreactive below pH 8. IAA is unstable under the light so reaction have to be carried out in dark. Adding DTT to the reaction mixture will quench the reaction of thiol-reactive probes. The thioether bond formed when an iodoacetic acid reacts with a protein thiol is very stable.⁴³

2.4.3. Maleimides

The thiol is added across the double bond of the maleimide to yield a thioether (Fig. 12).

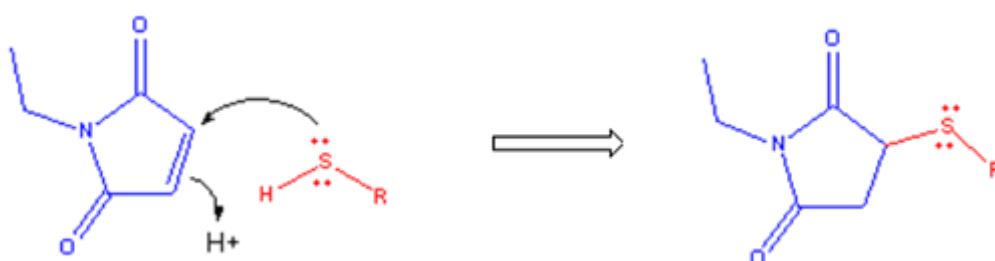


Figure 12. Reaction scheme of *N*-ethylmaleimide (NEM) with cysteine residue in the protein.⁴⁴

Reaction of maleimides with amines requires a higher pH than their reaction with thiols. Hydrolysis of the maleimide to an unreactive product can compete significantly with thiol modification, particularly above pH 8.

Once formed, maleimide-derived thioethers can hydrolyze to an isomeric mixture of succinamic acid adducts. Less frequently, they undergo cyclization with adjacent amines to yield crosslinked products.⁴³

2.4.4. Ellman's reagent

Ellman's reagent (5,5'-dithiobis-(2-nitrobenzoic acid), DTNB) is a widely used water-soluble reagent for spectrophotometric quantification of protein thiols. With thiols, it readily forms a mixed disulfide and releases the chromophore 5-mercapto-2-nitrobenzoic acid (TNB⁻) (Fig. 13). TNB⁻ in water dissociates further to TNB²⁻. Only accessible (surface-exposed) cysteines in a folded protein will be modified. Inaccessible ones can be quantified by carrying out the reaction in the denaturing conditions (presence of 6 M guanidinium chloride).⁴³

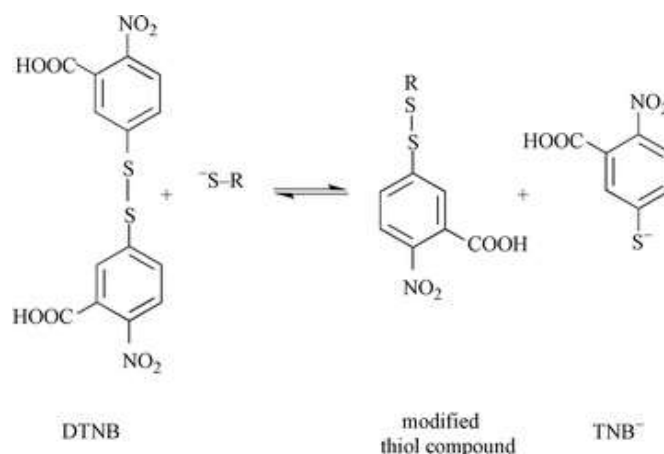


Figure 13. Reaction scheme of Ellman's reagent with cysteine residue in the protein.⁴⁵

2.4.5. 2-nitro-5-thiocyanobenzoic acid (NTCB)

Cleavage of proteins at cysteine residues following modification with 2-nitro-5-thiocyanobenzoate (NTCB) is a well-established procedure.⁴⁶⁻⁵¹ NTCB cyanylates reduced cysteine thiols at pH 8 (Fig. 14). The chain is then cleaved by cyclization under alkaline conditions. The N-terminus of the released peptide fragment becomes modified by the iminothiazolidine-carboxyl group during the cleavage reaction.^{46,47}

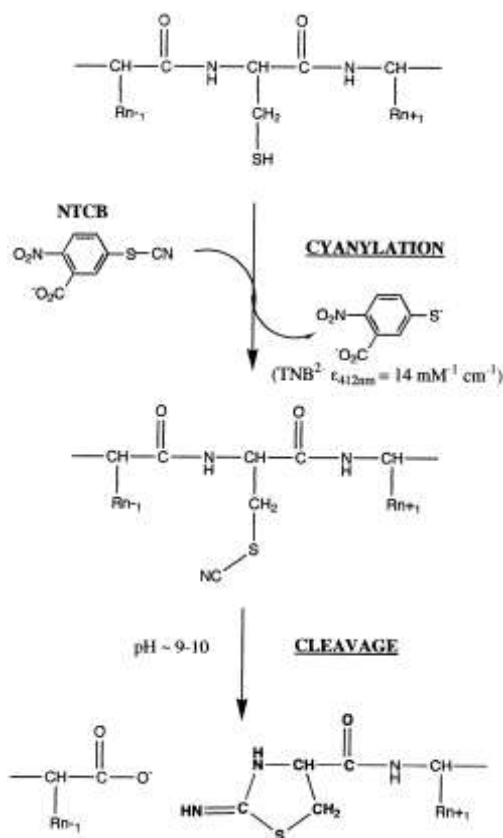


Figure 14. Reaction of 2-nitro-5-thiocyanobenzoic acid (NTCB) with cysteine residue in the protein releases coloured TNB²⁻ dianion. Cysteine gets cyanilated and protein gets cleaved on the N-terminal end of the modified cystein.⁵¹

The predominant reaction under these conditions is the cyanylation of the protein in the first step of the reaction, followed by cleavage (N-terminal to the cysteine) of the protein under alkaline conditions. Several side reactions are also possible, including β -elimination of the thiocyanoalanine residue instead of cyclization and cleavage⁴⁸ and the formation of mixed disulfides.⁴⁹ In order to favor the cyanylation reaction, a 10-fold molar excess of NTCB over total thiol groups are used at pH 8. Immediate acidification prevents most side reactions. Cyclization and cleavage of the peptide backbone is accomplished by raising the pH to 9.0 for a longer incubation period.

2.5. Mapping protein structure changes with cysteine labeling

Cysteine labeling has been used to study protein (un)folding, complex formation and conformational changes. The fundamental basis for the use of this approach is the change in the accessibility of particular cysteines for the reaction with electrophile, during the before mentioned processes.

Bernstein and colleagues have performed a native-state alkyl-proton exchange to monitor cysteines, in order to examine the folding landscape of *Escherichia coli* ribonuclease H.⁵² With the use of sulphhydryl reagents, Britto *et al.* have identified the most reactive cysteines in the rat brain tubulin, which were located nearby positively charged arginines and lysines.⁵³ More recently, Bogdanov *et al.* mapped the transmembrane protein topology by the substituted cysteine accessibility method (SCAM).⁵⁴ They have used thiol specific chemical reagents to study membrane protein topogenesis by substituted cysteine site-directed chemical labeling. Camerini *et al.* have used two alkylating agents to map the disulfide bridges in ovalbumin.

N-Ethylmaleimide was used to alkylate the reduced cysteines while IAM (iodoacetamide) alkylation was performed on gel after DTT reduction.⁵⁵ With the use of the similar approach, Cahudhuri *et al.* mapped disulfide bonds in tubulin.⁵⁶ By utilizing NTCB to cleave the protein next to the reduced cysteines, Daniel *et al.*⁵⁷ mapped the cysteines important for the zinc ion binding in *Escherichia coli* dihydroorotase. Burguete, Harbury and Pfeffer published a new method for the rapid identification of amino acid residues that contribute to protein-protein interfaces and they applied it on the tail interacting protein of 47 kDa (TIP47) which binds Rab9 GTPase and the mannose-6-phosphate receptors. They randomly incorporated cysteine mutations in TIP47 by expression in *Escherichia coli* cells harboring specific misincorporator tRNAs. The complex protected 48 cysteine probes from chemical modification by iodoacetamide. From this data a surface map of TIP47 has been derived, revealing the identity of surface-localized, hydrophobic residues that are likely to participate in protein-protein interactions. Direct mutation of predicted interface residues confirmed that the protein had altered binding affinity for the mannose-6-phosphate receptor.⁵⁸

§ 3. MATERIALS AND METHODS

3.1. Materials

3.1.1. Chemicals

2-Nitro-5-thiocyanobenzoic acid (NTCB) (Sigma), 5,5'-dithiobis-(2-nitrobenzoic acid) (DTNB) (Life technologies), acetic acid (100%, VWR), acetonitrile (Roth), ammonium bicarbonate (ABC) (Sigma), ampicilin (Roth), aprotinin (Genaxxon), complete-EDTA free protease inhibitors (Sigma), dithiothreitol (DTT) (Roth), ethanol (EtOH) (VWR), ethylenediaminetetraacetic acid (EDTA) (Sigma), formic acid (VWR), guanidine hydrochloride (GnCl) (Sigma), Hepes (Serva, analytical grade), hydrochloric acid (HCl, 32% pa) (VWR), imidazol (Roth), isopropyl β -D-1-thiogalactopyranoside (IPTG) (Roth), leupeptin (Genaxxon), Luria-Bertani (LB) medium powder (Serva), *N*-ethylmaleimide (NEM) (Thermo Fisher Scientific), pepstatin (Genaxxon), phenylmethylsulfonyl fluoride (PMSF) (Sigma), potassium acetate (VWR), sodium chloride (NaCl) (Sigma, research grade), Tris(hydroxymethyl)aminomethane (Tris) (Biozym)

3.1.2. Enzymes

Benzonase (Merck Milipore, 250 U/ μ L), lysozyme (Sigma, 70000 U/mg), trypsin (Sigma), His₆-TEV protease

3.1.3. Stock solutions

Ampicilin (100 mg/mL in 70% EtOH), IPTG (1 M), DTT (1 M), PMSF (100 mM in isopropanol), leupeptin (0.7 mg/mL in DMSO), pepstatin (1 mg/mL), aprotinin (1 mg/mL)

3.1.4. Buffers

All buffers were filtered through 0.22 μ m pore filter before use. Composition of buffers used:

HisA	50 mM Tris-HCl pH=7.4 300 mM NaCl
HisB	50 mM Tris-HCl pH=7.4 300 mM NaCl 400 mM Imidazole pH=7.4
Dialysis buffer	150 mM NaCl 15 mM Tris-HCl pH=7.4 1 mM DTT

MonoS A	15 mM Tris-HCl pH=7.4 1 mM DTT
MonoS B	15 mM Tris-HCl pH=7.4 1 mM DTT 2 M NaCl
GF buffer	50 mM Hepes KOH pH=7.6 0.2 mM EDTA 200 mM KOAc 10 mM DTT
Ellman buffer	50 mM Hepes KOH pH=7.6 0.2 mM EDTA 200 mM KOAc

3.1.5. *E. coli* strains

For protein expression, BL21 (DE3) strains were used. They contain the lambda DE3 lysogen which carries the gene for T7 RNA polymerase under the control of the lacUV45 promoter. IPTG is required to induce expression of the T7 RNA polymerase. The strains do not contain Lon and OmpT proteases. The lack of these two key proteases reduces degradation of heterologous proteins expressed in the cells.

3.2. Methods

3.2.1. Recombinant overexpression and purification of ATPase ISWI

Plasmid transformation

An aliquot of chemically competent cells (100 µL) was taken out of -80°C freezer and thawed on ice for 20 minutes. Agar plate with ampicillin was preheated in incubator to 37°C. To the thawed cells, 1 µL of plasmid DNA was added and mixed by flicking the tube with finger. The mixture of competent cells and plasmid DNA was incubated on ice for additional 20 minutes before heat shock (42°C, 45 seconds). The mixture was placed back on ice for two minutes and 250 µL of LB media without antibiotic was added. Cells were recovered in shaking thermoblock

at 37°C for one hour before plating on the agar plate with ampicilin. The plate was incubated over night at 37 °C.

Protein overexpression

LB media was prepared by adding 2 L of miliQ water to 40 g of LB powder and autoclaved for 10 minutes at 121 °C for 15 minutes. Single colony obtained from a fresh transformation was streaked on a new plate and incubated overnight at 37 °C.

Next day bacterial lawn from one plate was inoculated per 2 L of media. Cultures were grown at 37 °C with shaking until the OD600 (absorbance measured at 600 nm) reached 0.8, when they were induced with 1 mM IPTG (final concentration). The expression went overnight at 18 °C with shaking. Bacterial cultures were spun down (6000×g, 10 minutes, 4 °C), washed with cold water, flash frozen in liquid nitrogen and stored at -80 °C.

Cell lysis

To the frozen cell pellet were added: 15 µL DTT (final concentration 0.5 mM), 600 µL 1 M imidazole (final concentration 20 mM), 1 tablet complete-EDTA free protease inhibitors dissolved in 1 mL of HisA buffer, 300 µL PMSF (final concentration 1 mM), 30 µL each of leupeptin, pepstatin and aprotinin. Leupeptin and DTT were not added to the lysate which was used for cysteine alkylating reactions. Cells were thawed in the palm of a hand with occasional vortexing. As soon as thawed, the pellet was put back on ice and filled up to 30 mL with cold HisA buffer. Resuspended bacteria were cracked with 6 runs on Microfluidizer (pressure 1200 bar). Lysozyme was added (tip of a spatula) and cells were sonicated on ice (6× 10 seconds on, 10 seconds off, amplitude 25%). To the cell lysate 60 µL of benzonase was added and it was incubated for one hour on the rotating wheel in the cold room (4 °C).

Affinity chromatography

All purification steps were done in the coldroom. The lysate was centrifuged (19000 rpm, JA25.50 rotor, 4 °C, 30 min) and the supernatant was filtrated through 0.45 µm syringe filter. Column (HisTrap 5 mL, GE Healthcare) was equilibrated with 5% HisB buffer. Sample was loaded with sample pump at the flow rate 2.5 mL/min. Unbound sample was washed with 5% HisB (10 CV (column volumes)), 10% HisB (6 CV) and 20% HisB buffer (1 CV). ISWI was eluted with the flow rate 2 mL/min with a gradient 20-100% of HisB buffer in 10 CV. Eluted

fractions were analysed and pooled together. Concentration of eluted protein was measured and TEV protease was added (0.1 mg for every 8 mg of ISWI). Pooled fractions together with TEV protease were dialysed (Spectra/Por dialysis membrane, cut off 12000-14000 kDa) for 2 hours against 1 L of dialysis buffer and then overnight after buffer exchange. After dialysis, the sample was centrifuged (15 min, 6000×g, 4 °C). To remove His-tagged TEV protease, cleaved-off His-tag and uncleaved ISWI-TEV-6His, the second nickel-affinity chromatography was performed. Protein without tag will be present in the flowthrough. The same column was equilibrated in 10% of HisB buffer. The sample was loaded with sample pump at flow rate 1.5 mL/min. The column was washed from unbound sample with 10% of HisB buffer. During the sample loading and washing the flowthrough was collected in 1 mL fractions. The purity of fractions was analysed on SDS-PAGE.

Ion exchange

Conductivity of the sample was reduced below 10mS/cm by slow dilution with 2 volumes of 2% MonoS B buffer. The sample was mixed constantly during the dilution and at the end it was filtered through 0.2 µm syringe filter. MonoS column (5/50 GL GE Healthcare 1 mL) was equilibrated with 2% MonoS B. The sample was loaded with the sample pump at the flow rate 1 mL/min. Flow through was collected in 1.5 mL fractions. The protein was eluted with 2-30% MonoS B (10 CV) and 30-100% MonoS B (4 CV) and 0.5 mL fractions were collected and analyzed on SDS-PAGE.

Size exclusion chromatography

ISWI containing fractions were pooled and concentrated on the protein concentration unit to the 5 mL volume. The sample was then loaded onto the HiLoad Superdex200 (GE Healthcare, 120 mL) exclusion column equilibrated with GF buffer. The size exclusion was performed at the flow rate 0.5 mL/min and 1 mL fractions were collected and analyzed by SDS-PAGE. Fractions containing ISWI were pooled and the protein was concentrated to 5 mg/mL and 5 µL aliquots were flash frozen in liquid nitrogen to be stored at -80°C.

Sodium dodecyl sulfate polyacrylamide gel electrophoresis (SDS-PAGE)

Protein samples were mixed with 5×SDS loading dye ($w = 5\%$ β-mercaptoethanol, $w = 0.02\%$ bromophenol blue, $\varphi = 30\%$ glycerol, $w = 10\%$ SDS, 250 mM Tris-HCl, pH 6.8) and if needed

diluted with water. They were heated at 95 °C for 3 minutes. Samples from bacteria lysates were always vigorously vortexed to shear DNA. Prepared samples were loaded on precast SDS gels (Serva). All samples were analyzed on 8% gels, except for the NTCB cleavage reactions when 4-20% gradient gel was used. The electrophoresis was run in SDS running buffer (25 mM Tris, 192 mM glycine, $w = 0.1\%$ SDS) (150 V, BioRad Power Pac 300 electrophoresis power supply) in the XCell Sure Lock (Invitrogen) gel chamber, until the dye has ran out. The gel was rinsed with distilled water and stained in the staining solution (1 g dm⁻³ Coomassie Brilliant Blue R-250, $\varphi = 50\%$ methanol, $\varphi = 10\%$ glacial acetic acid). To speed up the staining, the staining solution was heated to the boiling and the gel was incubated for 5 minutes with shaking. After staining, the gel was boiled with distilled water to destain and the image was taken on ChemiDoc Imaging System (Biorad).

In one instance (Fig. 17), the 8% precast stain-free gel (Biorad) was used. The electrophoresis was run in Mini-Protean Tetra Cell gel chamber (Biorad) on 200 V until the dye has ran out. The gel contains the trihalo compounds which react with tryptophan residues in a UV-induced reaction to produce fluorescence. Reaction (for 5 minutes) and subsequent imaging were done in ChemiDoc Imaging System (Biorad).

Silver staining

All of the steps were performed with gentle shaking. The gel was rinsed with 200 mL methanol ($\varphi = 50\%$) for 10 minutes and then with 200 mL of water for 10 minutes. The gel was incubated with 200 mL Na₂SO₃ ($w = 0.02\%$) for 1 minute and immediately rinsed two times with water for 1 minute. The gel was stained with 200 mL of chilled AgNO₃ ($w = 0.1\%$) for 20 minutes and rinsed with water two times for 1 minute. Developing was done with Na₂CO₃ ($w = 2\%$) + formaldehyde ($w = 0.04\%$) with intensive shaking. After 30 seconds the developing solution was replaced. The developing was stopped with acetic acid ($w = 5\%$), two times 3 minutes. The gel was rinsed one more time with the same solution and then stored in water.

Measuring protein concentration

The absorbance at 280 nm was measured on DeNovix DS-11 spectrophotometer. The protein concentration was calculated from Beer-Lambert law; path length = 1 mm, ϵ (ISWI) = 121865 M⁻¹ cm⁻¹; M (ISWI) = 118873.3 g mol⁻¹.

3.2.2. Removal of DTT

The DTT was removed in 4 different ways. First, by at least four serial dilution and concentration steps. On the 200 μ L of purified protein 4 mL of 10 mM Hepes-KOH pH = 7.6 was added. The protein was then concentrated again in the protein concentration unit (Milipore, 4 mL cut off 10 kDa or 50 mL cut off 40 kDa) until the volume decreased to around 100 μ L. The procedure was repeated three more times. Every time the new concentrating device was taken. Second, DTT was removed on the Micro Bio-Spin desalting column with Bio-Gel P-6. Third, prolonged dialysis with often frequent buffer exchange was employed (Slide-a-lyzer mini dialysis device, cut off 7 kDa, 50 μ L). As a last way of buffer exchange, the protein was loaded on gel filtration column Superdex200 INCREASE 10/300 GL (~20 mL, GE Healthcare) equilibrated with GF buffer lacking DTT. The parallel procedure was always performed with 10 mM DTT to assess the efficiency of removal.

3.2.3. Assays with Ellman reagent

All assays have been performed in 10 mM Hepes-KOH pH=7.6 with or without 6 M guanidinium chloride. The absorbance at 412 nm was measured in the spectrophotometer or the microplate reader (PowerWave HT).

3.2.4. Reaction with NTCB

After the DTT removal, NTCB was added to 2 μ g of protein in 10-fold molar excess. NTCB was always freshly dissolved in 20 mM Hepes-KOH pH=7.6. The mixture was incubated at 40 °C for 20 minutes. The pH was then adjusted to 9 with 10 mM NaOH and the sample was incubated at 50 °C for one hour. The sample was then analyzed with SDS-PAGE.

3.2.5. Reaction with alkylating reagents

Reactions with NEM and IAA were performed at 18 °C. The reaction was stopped by adding the same amount of DTT. The samples were incubated at 56 °C for 30 minutes. The protein was treated with the secondary alkylating reagent (45 minutes, room temperature). Reaction with IAA was always performed in dark. 300 ng of trypsin was then added per 1 μ g of ISWI and incubated overnight at 37 °C. The samples were acidified with formic acid and the peptide desalting was performed as for in gel digestion.

3.2.6. Mass spectrometry

The prepared samples were measured by the mass spectrometry facility on the LTQ Orbitrap and analysed with MaxQuant software.

3.2.7. Cysteine mapping in bacterial lysate

Alkylation of cysteines in cell lysate

Cell lysate of *E. coli* cells overexpressing ISWI (400 μ L), obtained as described in section 3.2.1., was mixed with 1 μ L of NEM (2 M). Two reactions were prepared and incubated with shaking (750 rpm) in thermoblock at 4 °C and 18 °C, respectively. At two time points (10 min and 30 min) 15 μ L of reaction was mixed with 5 μ L of 5 \times SDS loading buffer supplemented freshly with DTT. Another set of reactions was prepared the same way, with the prior incubation of sample with 0.5 mM DTT.

Destaining of the gel bands

After staining, the gel was rinsed with distilled water and the bands of interest were individually cut out of it. Each gel band was cut in small pieces and the gel cubes were transferred in an 1.5 mL Eppendorf vial and incubated in water (100 μ L) for 5 minutes at room temperature. Supernatant was removed and to the cubes was added 200 μ L of 100 mM ammonium bicarbonate (ABC). After incubation for 5 minutes at room temperature, supernatant was removed. Gel cubes were incubated with 200 μ L of $\varphi = 50\%$ acetonitrile (ACN)/ 50 mM ABC for 30 minutes in the thermoblock at room temperature with shaking. The supernatant was removed and this step repeated if the gel cubes were still very blue. Finally, gel cubes were dried by addition of 100 μ L 100% ACN. Supernatant was removed.

Reduction and alkylation of disulfides

To the gel cubes 30 μ L of 2 mM DTT in 100 mM ABC was added and incubated for 30 minutes at 56 °C in thermoblock with shaking. Supernatant was removed and 30 μ L of 10 mM iodoacetic acid in 100 mM ABC was added and incubated for 45 minutes in the dark (room temperature). Supernatant was removed and gel cubes were washed with 200 μ L of 100 mM ABC with incubation for 5 minutes at room temperature. After removal of supernatant, 200 μ L

of 50% ACN/ 50 mM ABC was added to the gel cubes and they were incubated for 5 minutes in the shaker at room temperature. Supernatant was removed and gel cubes were dried with 100 μ L of 100% ACN.

In-gel tryptic digestion

Trypsin was dissolved in 25 mM acetic acid (AcOH) to 250 ng/ μ L and kept on ice. Solution of trypsin of 25 ng/ μ L was prepared in 100 mM ABC on ice and 10 μ L was added to the gel cubes followed by 15 minutes incubation on ice to allow them to soak in trypsin. Supernatant was then removed, 40 μ L of 100 mM ABC was added to cover the gel cubes and incubated at 37 °C for 12 hours.

Peptide extraction

To acidify the sample and to stop trypsin activity, formic acid (FA) was added to reach a final concentration of 5% in the solution. Sample was incubated in the sonication bath for 10 minutes. Supernatant was transferred to a fresh vial. To the gel cubes was added 40 μ L of 0.1% FA in 30% ACN and they were incubated in the sonication bath for 10 minutes. Supernatant was combined with the supernatant from tryptic digestion. This step was repeated one more time and the sample was dried in speedvac before further processing.

Peptide desalting

Solid-phase extraction (SPE) on stage tips was used to remove small molecules, buffer components and salts which interfere with reliable and reproducible identification of peptides. From the EMPORE PS-DVB disc material three discs were stamped per SPE column and placed into the end of a 200 μ L eppendorf tip. The tip with discs was placed in an empty eppendorf tube. The material was washed with 70 μ L methanol, twice with 70 μ L of FA ($\varphi = 0.1\%$) / ACN ($\varphi = 70\%$) and 4 times with trifluoroacetic acid (TFA) ($\varphi = 0.1\%$). Before washing with TFA, the column was placed into a fresh tube as well as before loading the sample and elution. The sample was loaded and washed 2 times with 50 μ L of FA ($\varphi = 0.1\%$). Desalted peptides were eluted by washing the column 2 times with 70 μ L of ACN ($\varphi = 70\%$) / FA ($\varphi = 0.1\%$). The sample was completely dried in the speedvac and reconstituted in (T)FA ($\varphi = 0.1\%$).

In silico tryptic digest

In silico tryptic digest has been performed with online PeptideCutter tool (Expasy).

§ 4. RESULTS AND DISCUSSION

4.1. Cysteine mapping in purified ATPase ISWI

4.1.1. Purification of ATPase ISWI

Full length sequence of ATPase ISWI (*D. melanogaster*) was previously cloned in our laboratory (backbone presumably pProExHT). On 5'-end the protein sequence was fused with the sequence coding TEV-protase cleavage site and 6xHis-tag. The plasmid was cloned in BL21(DE3) *E. coli* strain and overexpressed from 6 liters of culture. As tested by SDS-PAGE, the protein was expressed in a good yield (Fig. 15).

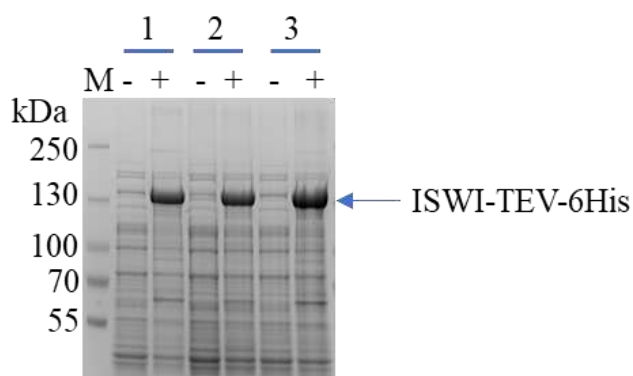


Figure 15. *E. coli* 2 L cultures (1, 2 and 3) expressing ISWI-TEV-6His, before and after induction with IPTG.

ISWI was N-terminally tagged with 6 histidines and it was purified from the cell lysate by nickel affinity chromatography (Fig. 16).

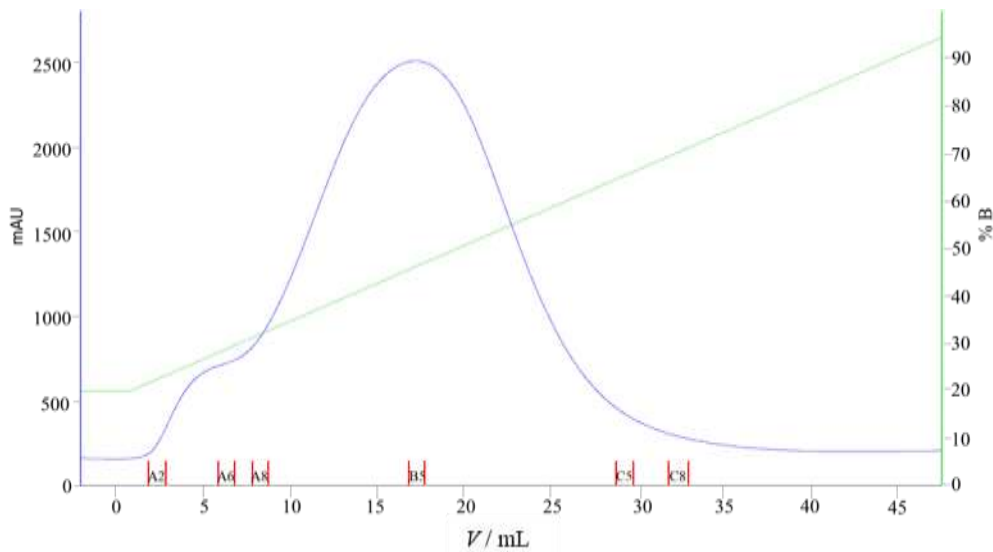


Figure 16. Nickel affinity purification of ISWI-TEV-6His from the cell lysate. The green line represents the imidazole gradient. ISWI elutes with approximately 120 mM imidazole. The fractions tested with SDS-PAGE are marked on the chromatogram. mAU = absorbance \times 1000

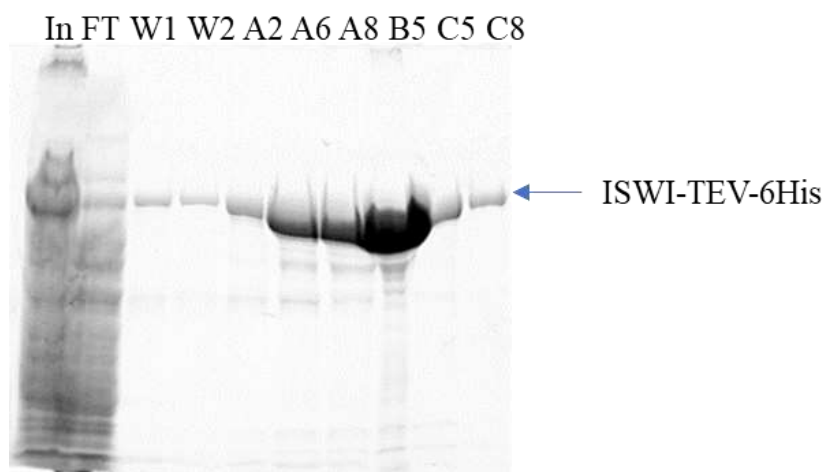


Figure 17. SDS-PAGE gel after nickel-affinity purification. Input (In), flow through (FT), wash fractions (W1 and W2).

Fractions were analyzed by SDS-PAGE gel (Fig. 17). Most of the proteins from the lysate do not bind to the resin, but there is also ISWI present in the flow through (FT). Some of the ISWI also elutes during washing of unspecifically bound proteins (W1 and W2). Earlier fractions before the big main peak also contain ISWI, but they might be partially oxidized species, due to the absence of reducing agent from the buffers. The fractions corresponding to the main peak were pooled together and incubated with TEV-protease. TEV-protease was also His-tagged.

ISWI was purified from the tag, the TEV protease and uncleaved His-tagged ISWI by second nickel affinity chromatography which will retain aforementioned impurities (Fig. 18).

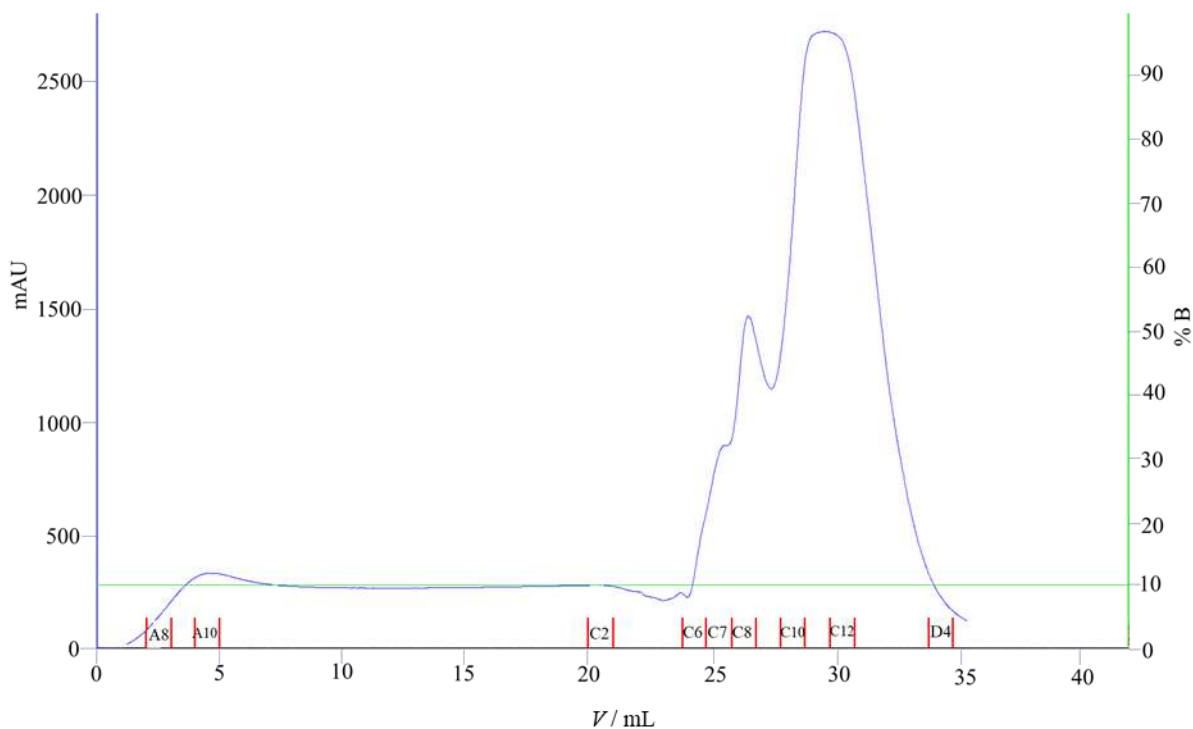


Figure 18. Second nickel affinity chromatography after TEV-cleavage. The fractions tested with SDS-PAGE are marked on the chromatogram.

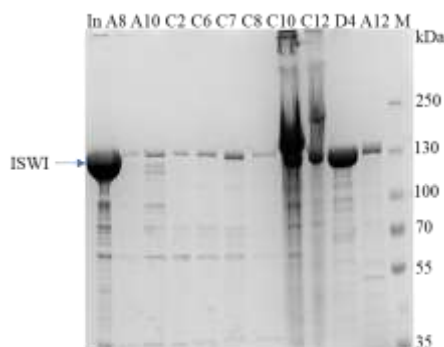


Figure 19. SDS-PAGE gel of eluted fractions after second nickel chromatography. In = input; M = protein marker. Sample C12 was over-cooked.

The fractions were analysed on the SDS-PAGE (Fig. 19). Most of the ISWI unspecifically binds to the resin and it is washed down after loading (fractions C10-D4). It is also present in the flow through (fractions A8-C3). It can also be seen that the TEV-protease reaction was not complete (fraction A12), but the tag was cleaved off from the majority of the protein.

In the next step, the protein was purified on the cationic exchange resin used. Conductivity of the sample was slowly decreased with constant mixing, to prevent aggregation and precipitation of the protein. Although the protein has the negative net charge, it will not bind on the MonoS resin if the ionic strength is too high. Some of the protein has precipitated during the dilution. Flow trough was collected for the case that ISWI does not bind on the resin. The ISWI peak always contains smaller or bigger shoulder which was not pooled together with main peak fractions (Fig. 20). The fractions were analysed on SDS-PAGE (Fig. 21). The pooled fractions were concentrated and loaded on size exclusion column (Fig. 22). After analysis on SDS-PAGE (Fig. 23), the fractions containing the pure ISWI were pooled together and concentrated. From 6 L of bacterial culture can be obtained up to 40 mg of the very pure protein.

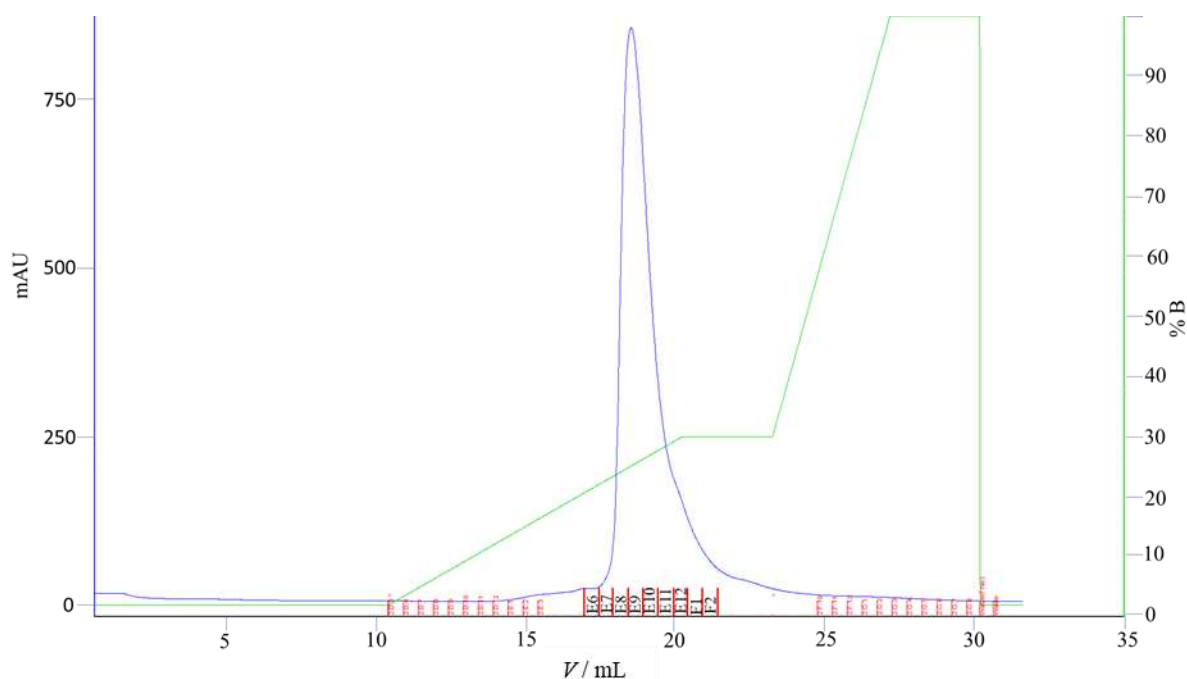


Figure 20. Chromatogram of anionic exchange purification (MonoS). The green line represents the percentage of % of buffer B used (2 M) in the mix with no-salt buffer. The ISWI was loaded with 40 mM salt and it starts eluting with 400 mM salt. The fractions tested with SDS-PAGE are marked on the chromatogram.

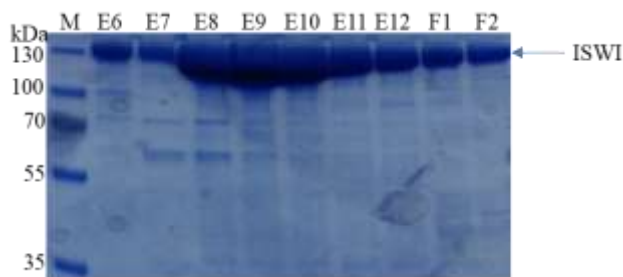


Figure 21. SDS-PAGE gel for fractions from MonoS purification. M = protein marker.

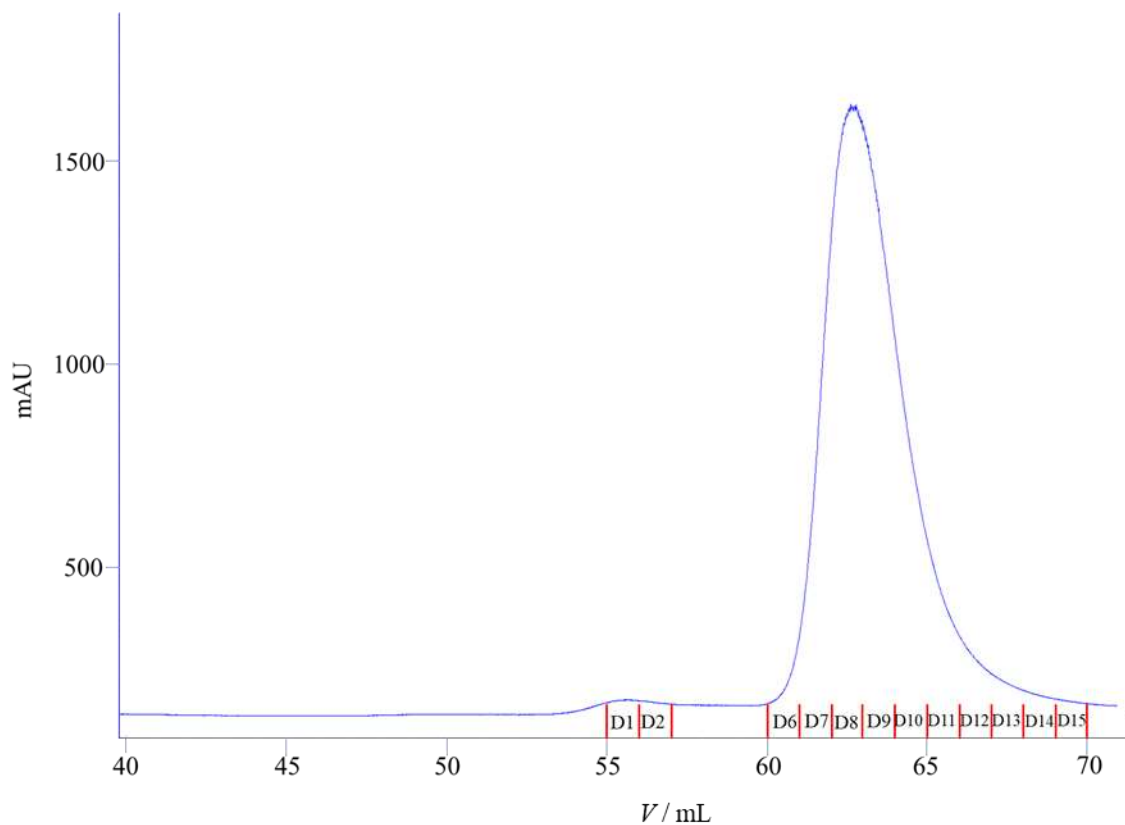


Figure 22. Chromatogram of size exclusion chromatography (S200), final step of ISWI purification. ISWI starts eluting from 60 mL. The fractions tested with SDS-PAGE are marked on the chromatogram.

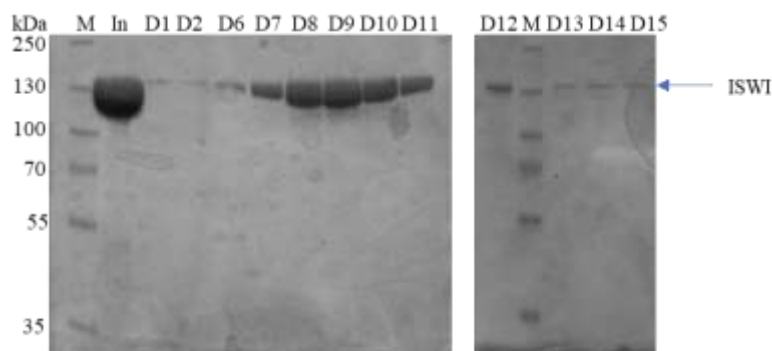


Figure 23. SDS-PAGE analysis of fractions eluted from size exclusion chromatography.

4.1.2. Determination of the molar extinction coefficient of 2-nitro-5-thiobenzonate dianion

The wavelength for which the absorbance (λ_{\max}) of 2-nitro-5-thiobenzonate dianion (TNB^{2-}) is maximal, was reported to be anywhere between 410 nm – 422 nm.⁴⁶ For that reason, the λ_{\max} has been experimentally determined under the conditions of the assay. In Ellman buffer, both with and without guanidinium-chloride, λ_{\max} is 412 nm (Fig. 24).

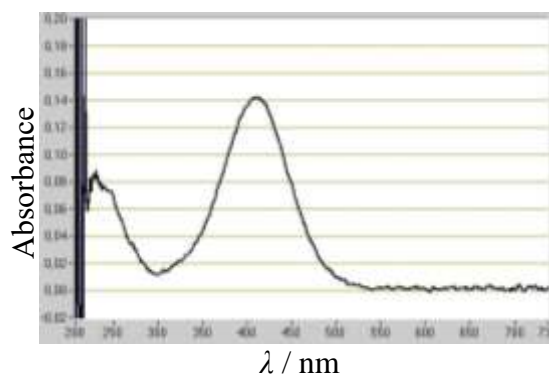


Figure 24. Determination of λ_{\max} of TNB^{2-} in Ellman buffer.

Molar extinction coefficient in Ellman buffer with and without guanidinium-chloride at 412 nm was then determined. Absorbance of solutions with various cysteine concentrations mixed with large excess of Ellman reagent has been measured. The absorbance values were measured after 5 minutes of incubation (Table 1) and did not differ significantly from repeated measurements after half an hour.

Table 1. Absorbance of solutions with different cysteine content and excess of Ellman reagent (60 mM) +/- guanidinium-chloride at 412 nm. Data plotted in Fig. 25.

c(cysteine)/ μM	A_{412} / nm	$A_{412} / \text{nm} (+\text{GnCl})$
5	0.151	0.141
10	0.290	0.277
15	0.416	0.425
20	0.554	0.554
25	0.712	0.695
30	0.806	0.821
35	0.960	0.934
40	1.067	1.076
45	1.178	1.194
50	1.293	1.306
55	1.383	1.379
60	1.476	1.483

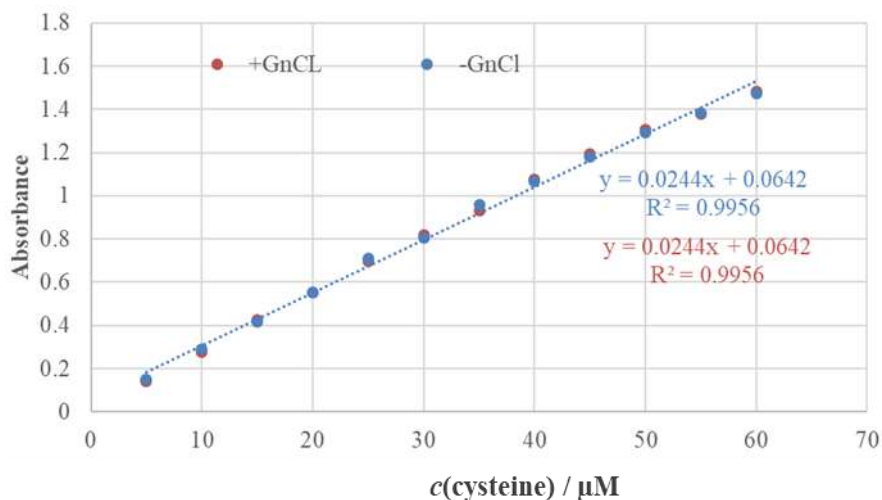


Figure 25. Determination of molar extinction coefficient for TNB^{2-} , $\lambda=412$ nm. Data shown in Table 1.

Absorbance depends linearly on cysteine concentration (Fig. 25). Molar extinction coefficients were determined from Beer-Lambert law:

$$A = c\epsilon l$$

The path length was 1 cm and ϵ was calculated from the slope of the equation for the fitted linear curve to be $24400 \text{ M}^{-1} \text{ cm}^{-1}$. These measurements were done in the large excess of DTNB (Ellman reagent). However if the kinetics of the reaction will be followed, the reaction is usually slowed down by using limiting or equimolar amounts of Ellman reagent.

The determination of the extinction coefficient was therefore repeated with the varying concentrations of cysteine standard, but with few different and smaller concentrations of Ellman reagent (Table 2). The absorbance is still dependent on concentration of cysteine in a linear fashion (Fig. 26). On the other hand, the calculated molar extinction coefficients (Table 3) were two times less than determined before. This could be explained by the shifting of chemical equilibrium towards the (products) coloured dianion (TNB^{2-}) caused by large excess of addition of Ellman reagent (reactant). It is also possible that there is a contribution from the absorbance of DTNB in such a large concentration. For the quantification of thiols, conditions of the first assay might be used. Direct and indirect influences of total concentration of Ellman reagent on the molar extinction coefficient must be kept in mind.

Table 2. Absorbance of solutions with different cysteine content and different total concentrations of Ellman reagent at 412 nm. Data plotted in Fig. 26.

	$c(\text{DTNB}) / \mu\text{M}$				
	60	90	120	150	180
$c(\text{cysteine}) / \mu\text{M}$					
2	0.021	0.025	0.027	0.026	0.021
5	0.061	0.065	0.059	0.065	0.071
7	0.083	0.089	0.084	0.072	0.075
10	0.123	0.122	0.121	0.107	0.118
15	0.185	0.185	0.184	0.174	0.183
20	0.243	0.242	0.226	0.248	0.239
30	0.368	0.373	0.362	0.341	0.366
40	0.489	0.481	0.479	0.469	0.482
50	0.606	0.602	0.596	0.587	0.594
60	0.741	0.716	0.715	0.697	0.722

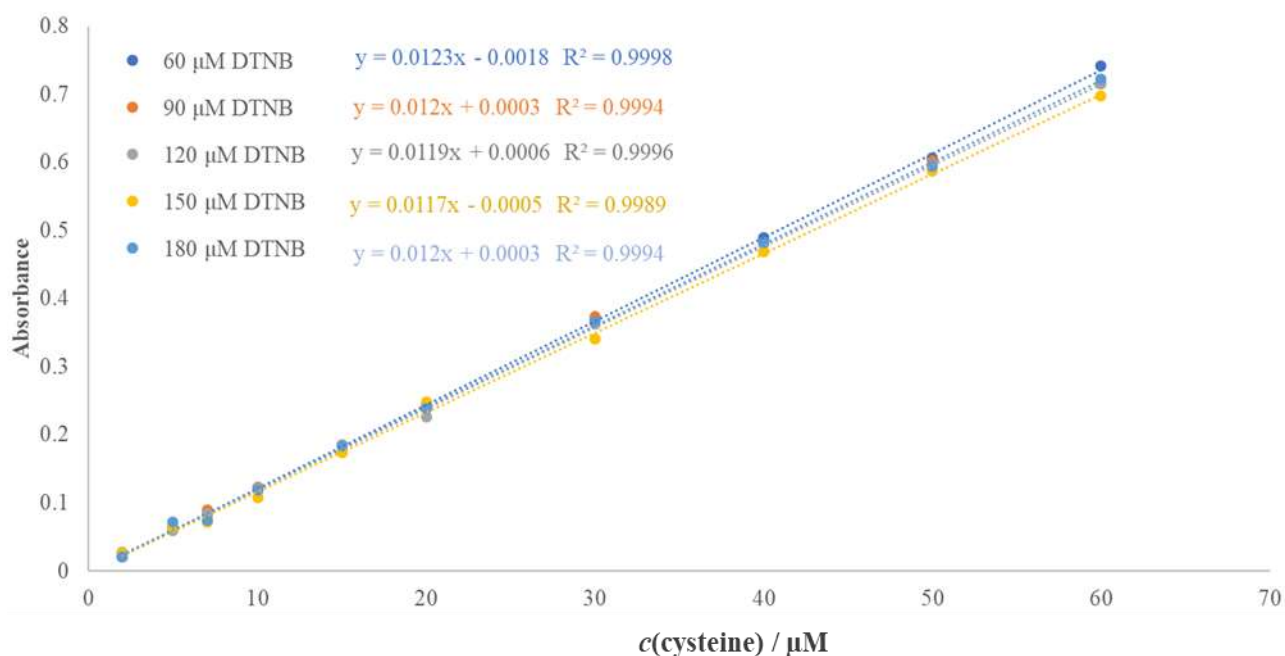


Figure 26. Determination of molar extinction coefficient for TNB^{2-} , $\lambda=412$ nm. Data shown in Table 2.

Table 3. Calculated molar extinction coefficients for TNB²⁻ at $\lambda=412$ nm for different total concentrations of Ellman reagent.

$c(\text{DTNB}) / \mu\text{M}$	$\varepsilon / \text{M}^{-1} \text{cm}^{-1}$
60	12300
90	12000
120	11900
150	11700
180	12000

From the measured absorbance values for cysteine in different concentrations, something as well can be concluded about the sensitivity of the assay. To get the reliable measurements, cysteine concentration has to be at least 5 μM .

4.1.3. Adapting the assay for the smaller quantities of analyte

At this point, the assay requires 5 μM protein in the total volume of 1 mL. In total, 5 nmol is needed for only one replicate, corresponding to 0.6 mg of ISWI. This is a significant amount of protein, so the assay was adapted to be performed in 384-well plate and absorbance measured in the microplate reader. Two reaction volumes were tested – 30 and 100 μL . When only 30 μL of reaction was used, the read out was not precise for cysteine concentrations lower than 20 μM (Table 4; Fig. 24). For that reason, the volume was increased to 100 μL . When the 100 μL of reaction was used, the absorbance/concentration relation was linear even at the lowest cysteine concentrations (Table 5; Fig. 25).

Table 4. Absorbance measurements for different cysteine concentrations. Three different total DTNB concentrations were used in total reaction volume 30 μL . $\lambda = 412$ nm. Data plotted in Fig. 24.

	c (cysteine) / μM									
	2	5	7	10	15	20	30	40	50	60
$c_0(\text{DTNB}) / \mu\text{M}$										
60	0.017	0.012	0.019	0.025	0.041	0.06	0.093	0.129	0.154	0.187
90	0.01	0.013	0.022	0.03	0.043	0.059	0.092	0.12	0.152	0.182
180	0	0.011	0.026	0.033	0.039	0.06	0.087	0.117	0.146	0.179

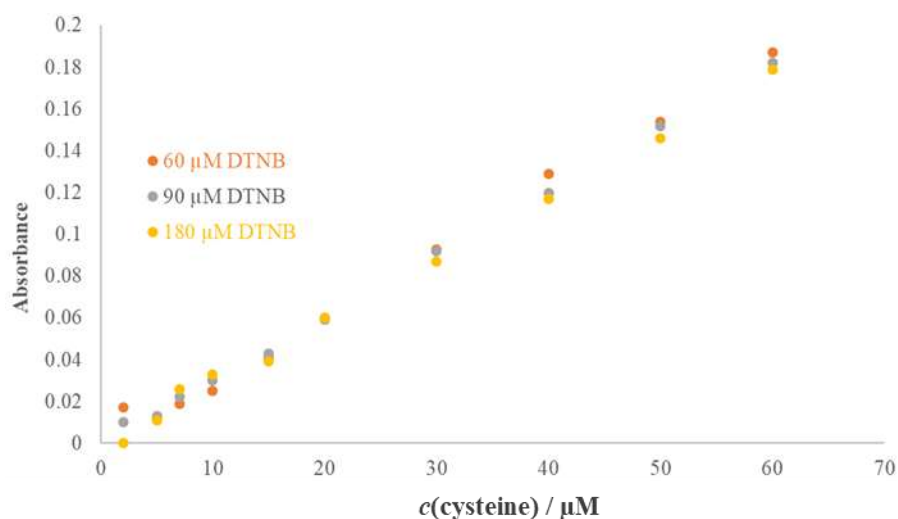


Figure 24. Absorbance measurements plotted against corresponding cysteine concentrations. Three different total DTNB concentrations were used in total reaction volume 30 μL . $\lambda = 412$ nm. Data shown in Table 4.

Table 5. Absorbance measurements for different cysteine concentrations. Three different total DTNB concentrations were used in total reaction volume 100 μL . $\lambda = 412 \text{ nm}$. Data plotted in Fig. 25.

	$c(\text{cysteine}) / \mu\text{M}$									
	2	5	7	10	15	20	30	40	50	60
$c_0(\text{DTNB}) / \mu\text{M}$										
60	0.009	0.038	0.060	0.084	0.140	0.183	0.278	0.369	0.459	0.560
90	0.008	0.039	0.053	0.089	0.125	0.177	0.270	0.365	0.448	0.544
180	-0.001	0.030	0.056	0.073	0.120	0.181	0.261	0.357	0.443	0.537

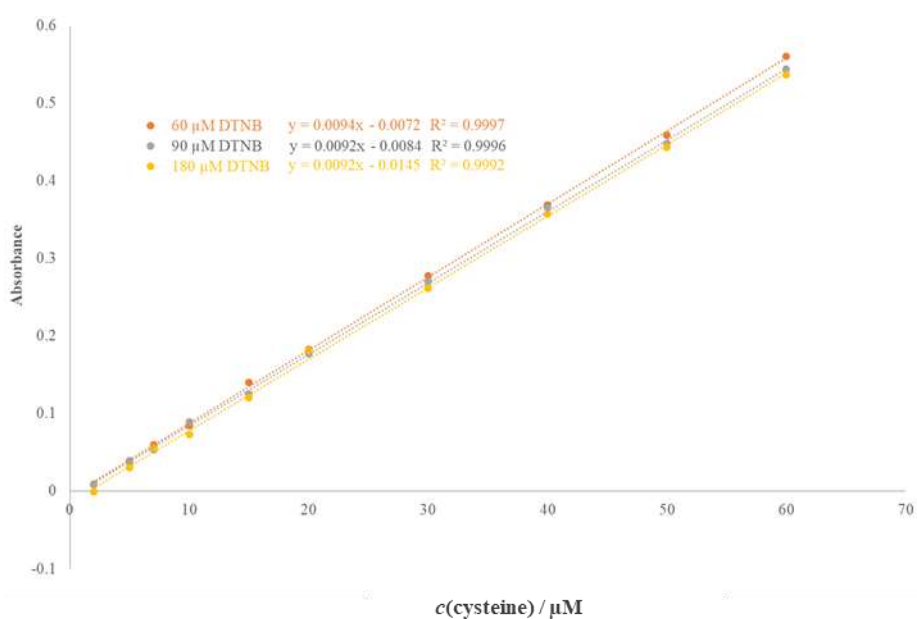


Figure 25. Absorbance measurements plotted against corresponding cysteine concentrations.

Three different total DTNB concentrations were used in total reaction volume 100 μL . $\lambda = 412 \text{ nm}$. Data shown in Table 5.

The path length was calculated from the experimental data (the slope of absorbance read outs for different cysteine concentrations) with the use of previously determined extinction coefficients (Table 3). For all three DTNB concentrations used, the same value for the path length was obtained (Table 6), which is the indicator of the correct methodological approach and reliable measurements.

Table 6. The calculated path length l for three different total concentrations of Ellman reagent in 384-well plate, $V = 100 \mu\text{L}$.

$c(\text{DTNB}) / \mu\text{M}$	$\varepsilon / \text{M}^{-1} \text{cm}^{-1}$	$\varepsilon \times l / \mu\text{M}^{-1}$	l / cm
60	12300	0.0094	0.76
90	12000	0.0092	0.77
180	12000	0.0092	0.77

4.1.4. Reaction of the ATPase ISWI with Ellman reagent

ISWI (5 μM) was mixed with the solution containing Ellman reagent (60 μM), after the initial absorbance has been measured. The reaction was followed over 30 minutes (Fig. 26). The end point of the reaction is higher than expected (0.5) and the absorbance is still growing. This is because ISWI precipitates during the reaction with Ellman reagent. The precipitation is probably caused with the disturbance of the native protein folding during intercalation of a big aromatic ring. The precipitation did not occur when the reaction was performed under denaturing conditions (6 M GnCl).

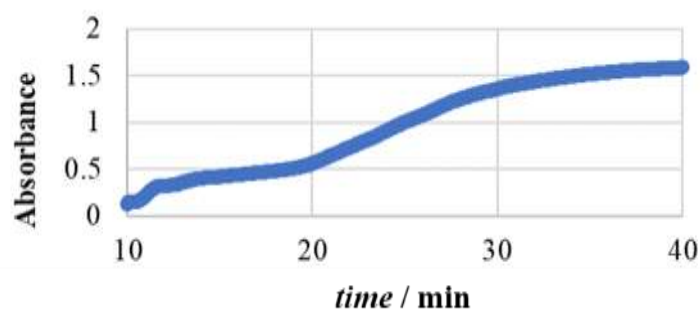


Figure 26. The absorbance measurements ($\lambda = 412 \text{ nm}$) during ISWI reaction with Ellman reagent.

4.1.5. Reaction of ISWI with 2-nitro-5-thiocyanatobenzoic acid

In the contrast to Ellman reagent, the precipitation did not occur when the reaction was performed with 2-nitro-5-thiocyanatobenzoic acid (NTCB) which adds to cysteines only small cyano group. The absorbance during the reaction of the ISWI with NTCB has also been measured, but in all cases, the residual DTT content was significant enough to make the interpretation of the results impossible.

The reaction was then analyzed on the SDS-PAGE after the cyanylation and cleavage (Fig. 27). On the gel it is visible that the ISWI was fully degraded. After silver staining, many bands in the lower part of the gel became visible.

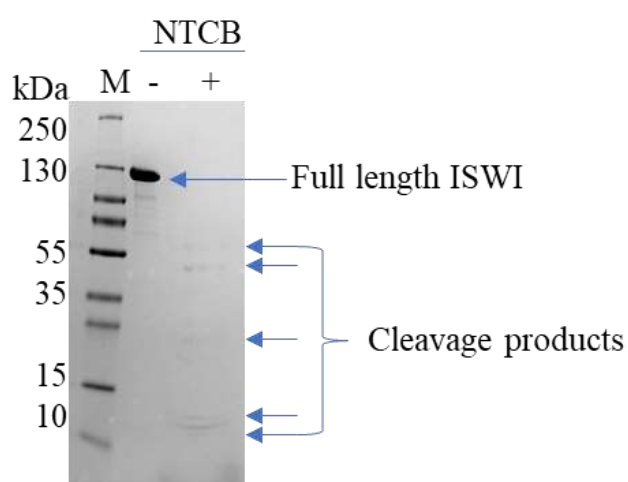


Figure 27. The SDS-PAGE after treating ISWI with NTCB followed by NaOH-catalyzed cleavage.

4.1.6. Reaction of ISWI with iodoacetic acid and *N*-ethylmaleimide

The alkylation reaction with iodoacetic acid (IAA) and *N*-ethylmaleimide (NEM) was quenched and the extent of the reaction was analysed by cyanylation with NTCB and subsequent cleavage (Fig. 28).

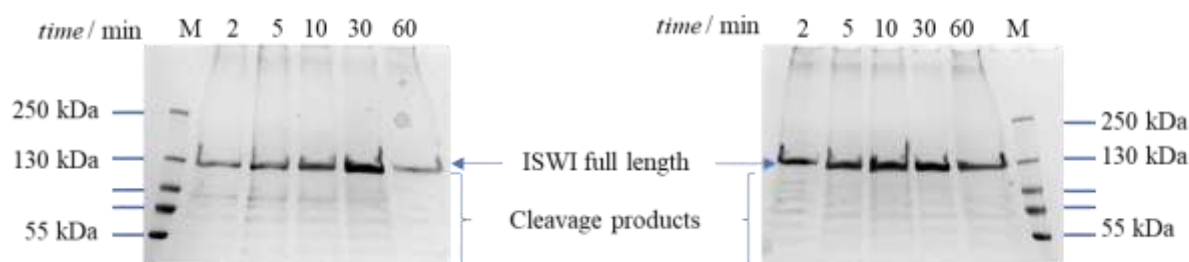


Figure 28. The SDS-PAGE after alkylation with IAA (left) and NEM (right) followed by cyanylation with NTCB and NaOH-catalyzed cleavage.

The cysteines which have reacted with IAA or NEM are protected from NTCB and cleavage. On the SDS-PAGE is visible that the ISWI is, in both cases, partially cleaved and it seems that the pattern and quantity of cleavage in each lane is the same. This can be due to the incomplete cyanylation or cleavage or both, but it has been shown that the reaction, with the same amounts of ISWI and NTCB, goes to the completion. The other possible explanation for this result is that the alkylation reaction is very fast, causing all exposed cysteines to react in the first minutes.

Upon addition of NaOH, all reactions gave strong yellow colour, originating from TNB²⁻. Probably the NTCB hydrolyses with increase in pH. After cleavage reaction, the reactions with NEM are still yellow, however reactions containing IAA became completely clear and colourless. With addition of SDS the precipitate is formed with the NEM-containing mixtures and the colour of SDS loading buffer changes from blue to the dark green. On the other hand, after cleavage is finished IAA-containing mixtures become a little yellow.

It is not simple to follow the kinetics of alkylation reactions. Therefore, as the last experiment in this approach, ISWI was incubated with substoichiometric amounts and excess (of primary alkylating reagent (NEM or IAA)). After the primary alkylation reaction, the protein was treated with the same amount (as of alkylating reagent) of DTT and heated to denature. After denaturation, the large excess of secondary alkylation reagent (IAA or NEM, respectively) was added. The samples were prepared for analysis by mass spectrometry.

Unfortunately, the trypsin digest of the samples did not go successfully and only one peptide with cysteine has been detected. Many unspecific cleavages have occurred. The reason for that is probably the change in pH during trypsin digest. Buffers with higher buffering capacity should be used next time.

4.2. Cysteine mapping in bacterial lysate

Reactions with alkylation reagents, which are performed before mass spectrometry, are very fast. Therefore it is very hard to selectively label exposed cysteines. We have tried to do this in the bacterial cell lysate obtained after ISWI overexpression and cell disruption. To identify which cysteines are inaccessible to alkylation reagents (buried in the inner protein structure), the lysate was treated with 5 mM of the primary alkylating reagent (NEM) and loaded on SDS-PAGE (Fig. 29).

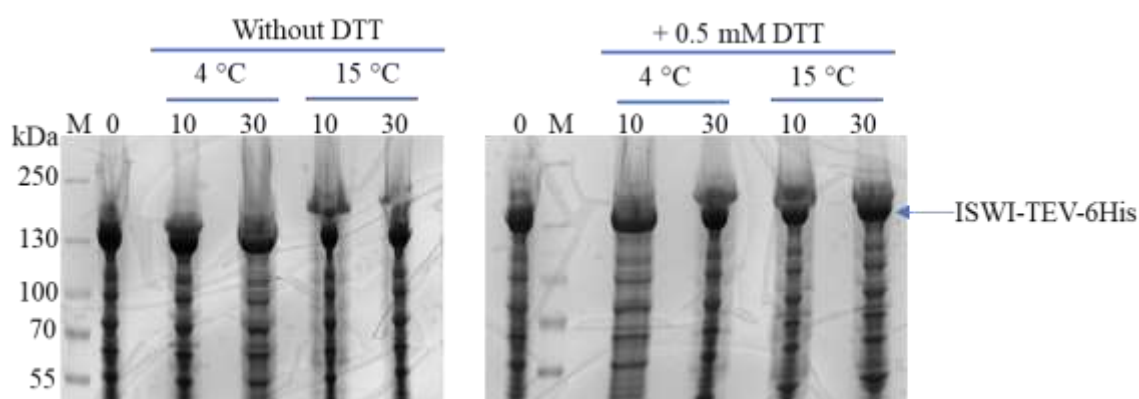


Figure 29. SDS-PAGE gel after treatment of cell lysate with 5 mM NEM, performed under four different conditions with three time points analysed (0, 10 and 30 minutes). There is no visible change. The bands corresponding to ISWI-TEV-6His were cut out from the gel and prepared for mass spectrometry.

Bands corresponding to the ISWI were excised from the gel and processed for mass spectrometry analysis. After denaturation (SDS, heating) and treatment with the excess of DTT, the samples were alkylated with secondary alkylating reagent (IAA) and digested with trypsin. Trypsin preferentially cleaves after arginine (R) and lysine (K) residues. The ATPase ISWI contains 11 cystein residues in total. *In silico* tryptic digest has predicted 10 cystein containing peptides (Table 7). Only peptides longer then 6 amino acids can be reliably detected by the analysis.

Table 7. Peptides after the *in silico* tryptic digest of ISWI.

Peptide sequence	Mass/Da	Position
LLITGTPLQNNLHELWALLNFLLPDVFNSSEDFDEWFNTNTCLGDDALITR	5848.9	281-331
CTNHPYLFDDGAEPGPPYTTDTHLVYNSGK	3194.5	404-432
DVLMPGEWDVCVTSYEMCIR	2346.0	221-240
MLDILEDYCHWR	1593.7	459-470
AVCLIGDQDTR	1190.6	205-215
CNTLITLIER	1175.6	956-965
CTELQDIER	1106.5	846-854
FLVCMLHK	990.5	909-916
NYNYCR	832.3	471-476
WCPSLR	761.4	199-204

Table 10. Cysteines containing modified peptides detected by mass spectrometry analysis (green). The intensities are given for each peptide.

	Peptide sequence	modification IAA NEM		without DTT				with DTT			
				4 °C		18 °C		4 °C		18 °C	
				10 min	30 min	10 min	30 min	10 min	30 min	10 min	30 min
Cys207	1 AVCLIGDQDTR	0	1	17366000	9947100	0	600230	10641000	11246000	2517300	3985500
	2 AVCLIGDQDTR	1	0	6810900	7892100	0	264740	8395400	30135000	1564500	1258300
Cys956	3 CNTLITLIER	0	1	201260000	9640200	86374	5098400	16489000	113570000	18332000	17406000
	4 CNTLITLIERENIELEEKER	0	1	0	0	0	87486	36344000	29403000	0	649150
Cys846	5 CTELQDIER	0	0	348160	0	0	0	44791	0	0	0
	6 CTELQDIER	0	1	1643700000	683660000	2093100	299110000	416390000	3361800000	1027600000	2447800000
	7 CTELQDIER	1	0	41597000	14934000	0	1119700	39442000	100260000	9939900	10610000
Cys404	8 CTNHPYLFDDGAEPGPPYTTDTHLVYNSGK	0	1	0	0	0	0	0	3192900	0	0
	9 CTNHPYLFDDGAEPGPPYTTDTHLVYNSGK	1	0	0	0	0	0	0	1862500	0	0
Cys231	10 DVLMPGEWDVCVTSYEMCIR	2	0	0	0	0	0	0	1027700	0	0
	11 DVLMPGEWDVCVTSYEMCIR	1	1	0	0	0	0	0	4184700	0	0
Cys238	12 DVLMPGEWDVCVTSYEMCIR	1	1	0	0	0	0	0	1715800	0	0
Cys404	13 KCTNHPYLFDDGAEPGPPYTTDTHLVYNSGK	1	0	130400	0	0	0	4255400	0	0	0
	14 MLDILEDYCHWR	1	0	0	66724	0	0	3485700	5160800	59390	0
Cys467	15 MLDILEDYCHWR	0	1	0	0	0	0	1271800	0	0	0
	16 NYTEIEDRFLVCMLHK	1	0	0	0	0	0	3552700	0	120110	0
Cys912	17 NYTEIEDRFLVCMLHK	0	1	0	0	0	0	5092400	0	152420	123360
Cys200	18 WCPSLR	1	0	0	0	0	0	0	2017500	0	0

Nine out of eleven cysteines have been identified in at least one sample. Cysteine-322 and cysteine-475 were not detected at all. Cysteine-322 is a part of the very big peptide (50 amino acids) which is probably too heavy to reach the detector. On the other hand, the peptide containing cysteine-475 is too small for reliable detection.

For the sample 18 °C 10 min without DTT very few peptides and with small intensities were recovered meaning that during the purification significant loss of the material has happened.

Generally in the lysates treated with DTT more peptides with modifications were detected. This might indicate the existence of disulfide bridges in ISWI in bacterial lysate. Surprisingly, it seems that alkylation reaction did not significantly improve with the extended time or higher temperature. The biggest peptide (containing the residues 404-433) was detected in only one sample due to its big mass and hydrophobicity. On the other hand, the shortest peptide (peptide 13) was detected in only one sample due to its very small size. To get the full coverage of all the cysteines, other methods of digest will be considered.

Peptides containing cysteine-207 have been detected in every sample with both of the modifications, although the peptide 1 has been detected with consistently higher intensities. This indicates that cysteine-207 is available for reaction in cell lysate, but is not completely exposed so that all cysteines-207 can react. Effects of DTT and prolonged reaction time on the intensity ratio of these two modifications are conflicted.

Cysteine-956 is alkylated with primary alkylating reagent (NEM) in all of the samples and under every condition. On the other hand, its modification with secondary alkylating reagent (IAA) has never been detected (peptides 3 and 4). This cysteine is probably exposed on the protein surface and it does not take part in disulfide bridges.

Cysteine-846 has been detected in three forms, however peptide 5 containing unmodified cysteine has been detected with very low intensities in all of the samples. NEM modification has been detected with the largest intensities in all samples (peptide 6) indicating that this residue is not buried inside the protein.

Peptides 13-18 have very poor coverage especially in the samples which were not treated with DTT. Cysteine-404 present in the long peptide 13 was detected only with IAA modification. Although intensities are not so bad, due to the detection in only two samples and the big size of the peptide, this result should not be overinterpreted.

Cysteine-467 was covered in only half of the samples, but the peptide modified with NEM (peptide 15) was either never detected or it was detected with three times smaller intensity when compared with peptide modified with IAA (peptide 14). This residue is probably buried in the interior of the protein and thus unavailable for the interaction with the primary alkylating reagent (NEM).

Cysteine-912 was prevalently detected in the peptide modified by NEM (peptide 17), but due to the detection in only few samples, this result should not be absolutely trusted.

The main conclusions from this experiment are summarized in Figure 30. The most exposed cysteines are located in the HSS domain. To get more confident results, the experiment will be repeated with different digestion techniques before mass spectrometry analysis, e. g. digestion with chymotrypsin or chemical cleavage will be used.

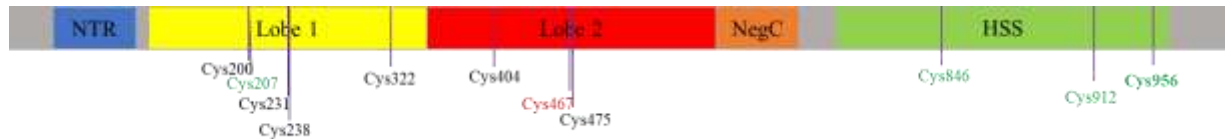


Figure 30. The ISWI domain structure with indicated cysteine locations. For the cysteines marked in black no confident information about exposure could be derived. Red coloured cysteines are most probably buried inside of the protein, while the green coloured cysteines are most likely exposed on the protein surface. In bold is the cysteine whose exposure can be assessed with high certainty.

§ 5. CONCLUSION

The ATPase ISWI, chromatin remodeler from *Drosophila melanogaster* has been probed with thiol-reactive probes to identify surface-exposed cysteines. The protein was purified with four step purification: nickel affinity chromatography, His₆-tag digestion and removal, ion exchange chromatography and size exclusion chromatography. The yield and purity of the protein after purification were very good. The required removal of DTT used during the purifications, lead to significant loss of the protein.

The reactions with thiol-reactive probes which give the coloured products and can be followed spectrophotometrically, were optimized to minimize the amount of analysed material. ISWI precipitated during the reaction with commonly used Ellman reagent (5,5'-dithiobis-(2-nitrobenzoic acid)), unless the reaction was performed under the denaturing conditions. The 2-nitro-5-thiocyanatobenzoic acid (NTCB), which introduces smaller cyano group on the cysteine residues, did not cause the precipitation of the protein. After cyanylation, cyanylated cysteines caused the peptide bond cleavage on the N-terminal end of the modified residue.

To identify surface exposed cysteines, ISWI was treated with an alkylating reagent. The extend of alkylating reaction could not be assessed with quenching and reaction with excess of NTCB, probably because alkylating reactions are very fast.

Finally, ISWI was treated with two different alkylating reagents. One before and one after denaturation. The two reactions add to the cysteines different modification groups which were then discriminated in mass spectrometer. In that way, the cysteines which are surface-exposed in the native protein structure could be identified. Half of the total cysteines could be clasified either as buried or surface-exposed in the protein structure. For this experiment protein purification was not required, as it can be done after overexpression and the bacterial cell lysis.

There is a very limited structural information on the remodelers. It appears that a remodeler undergoes a large conformational change upon engagement with the nucleosome substrate. For the ATPase ISWI, our lab recently applied the integrative structural biology approach to probe the ISWI structure in solution. The obtained model predicts that the C-terminal HAND-SAND-SLIDE (HSS) module packs against the ATPase domain through its SLIDE domain. To verify the model, we will apply results of this work to assess the change in cysteines accesibility upon

deletion of HSS domain. The change in the exposure (or the lack of) of the particular cysteines, will help us to judge the validity of the derived model.

§ 6. ABBREVIATIONS

DNA	Deoxyribonucleic acid
DTNB	5, 5'-dithiobis-(2-nitrobenzoic acid) = Ellman reagent
DTT	dithiotreitol
EDTA	Ethylenediaminetetraacetic acid
HEPES	4-(2-hydroxyethyl)-1-piperazineethanesulfonic acid
IAA	iodoacetic acid
IPTG	Isopropyl β -D-1-thiogalactopyranoside
mAU	mili absorbance units
NCP	Nucleosome core particle
NEM	<i>N</i> -ethylmaleimide
NTCB	2-nitro-5-thiocyanatobenzoic acid
OD	Optical density
PMSF	Phenylmethylsulfonyl fluoride
SDS-PAGE	Sodium dodecyl sulfate polyacrylamide gel electrophoresis
TEV	Tobacco Etch Virus
TRIS	Tris(hydroxymethyl)aminomethane

§ 7. LITERATURE

1. D. L. Nelson, M. M. Cox, *Lehninger principles of biochemistry*, W. H. Freeman, New York, 2008
2. R. K. McGinty, S. Tan, in (J.L. Workman and S. M. Abmayr, ed.) *Fundamentals of Chromatin*, Vol. 1, Springer, New York 2014, pp. 1-29.
3. J.D. McGhee, G. Felsenfeld G, *Annu. Rev. Biochem.* **49** (1980) 1115–1156.
4. <http://chemistry.umeche.maine.edu> (September 3th, 2017.)
5. J. A. Eisen, K. S. Sweder, P. C. Hanawalt, *Nucleic Acids Res.* **23** (1995) 2715–2723.
6. A. Flaus, D. M. A. Martin, G. J. Barton, T. Owen-Hughes, *Nucleic Acids Res.* **34** (2006) 2887–2905.
7. G. Längst, L. Manelyte, *Genes (Basel)* **6** (2015) 299–324.
8. P. Filippakopoulos, S. Knapp, *FEBS Lett.* **586** (2012) 2692–2704.
9. B.G. Wilson, C. W. M. Roberts, *Nat. Rev. Cancer* **11** (2011) 481–492.
10. B. Lemon, C. Inouye, D. S. King, R. Tjian, *Nature* **414** (2001) 924–928.
11. Z. Yan, *Genes Dev.* **19** (2005) 662–1667.
12. J. K. Sims, P. A. Wade, *Cell* **144** (2011)
13. V. Delmas, D. G. Stokes D.G, R. P. Perry, *Proc. Natl. Acad. Sci. U. S. A.* **90** (1993)
14. D. G. Stokes, R. P. Perry, *J. Mol. Biol.* **15** (1995) 2745–2753.
15. D. P. Ryan, R. Sundaramoorthy, D. Martin, V. Singh, T. Owen-Hughes, *EMBO J.* **30** (2011) 2596–2609.
16. A. A. Watson, P. Mahajan, H. D. Mertens, M. J. Deery, W. Zhang, P. Pham, X. Du, T. Bartke, W. Zhang, C. Edlich *et al.*, *J. Mol. Biol.* **422** (2012) 3–17.
17. M. Murawska, A. Brehm *Transcription* **2** (2011) 244–253.
18. T. Gkikopoulos, P. Schofield, V. Singh, M. Pinskaya, J. Mellor, M. Smolle, J. L. Workman, G. J. Barton, T. Owen-Hughes, *Science* **333** (2011) 1758-1760.
19. S. C. West, *Annu. Rev. Genet.* **31** (1997) 213–244.
20. X. Shen, G. Mizuguchi, A. Hamiche, C. Wu *Nature* **406** (2000) 541–544.
21. S. Wu, Y. Shi, P. Mulligan, F. Gay, J. Landry, H. Liu, J. Lu, H. H. Qi, W. Wang, J. A. Nickoloff *et al.*, *Nat. Struct. Mol. Biol.* **14** (2007) 1165–1172.
22. Y. Bao, X. Shen, *Cell* **144** (2011)

23. M. Papamichos-Chronakis, S. Watanabe, O. J. Rando, C. L. Peterson, *Cell* **144** (2011) 200–213.
24. X. Shen, R. Ranallo, E. Choi, C., *Mol. Cell* **12** (2003) 147–155.
25. T. Tsukuda, A. B. Fleming, J. A. Nickoloff, M. A. Osley, *Nature* **438** (2005) 379–383.
26. H. Van Attikum, O. Fritsch, S. M. Gasser, *EMBO J.* **26** (2007) 4113–4125.
27. C. R. Clapier, B. R. Cairns, *Annu. Rev. Biochem.* **78** (2009) 273–304.
28. R. Strohner, A. Nemeth, K. P. Nightingale, I. Grummt, P. B. Becker, G. Längst, *MCB.* **24** (2004) 1791–1798.
29. J. Li, G. Längst, I. Grummt, *EMBO J.* **25** (2006) 5735–5741.
30. R. Santoro, J. Li, I. Grummt, *Nat. Genet.* **32** (2002) 393–396.
31. C. R. Clapier, B. R. Cairns, *Nature* **492** (2012) 280–284.
32. R. Deuring, L. Fanti, J. A. Armstrong, M. Sarte, O. Papoulas, M. Prestel, G. Daubresse, M. Verardo, S. L. Moseley, M. Berloco, T. Tsukiyama, C. Wu, S. Pimpinelli, J. W. Tamkun, *Mol. Cell* **5** (2000) 355–365.
33. F. Müller-Planitz, H. Klinker, J. Ludwigsen, P. B. Becker, *Nat. Struct. Mol. Biol.* **20** (2013) 82–89.
34. W. Dang, M. N. Kagalwala, B. Bartholomew, *Mol. Cell Biol.* **26** (2006) 7388–7396.
35. T. Grüne *et al.*, *Mol. Cell* **12** (2003) 449–460.
36. S. K. Hota *et al.*, *Nat. Struct. Mol. Biol.* **20** (2013) 222–229.
37. J. Ludwigsen, H. Klinker, F. Mueller-Planitz, *EMBO Rep.* **14** (2013) 1092–1097.
38. L. Yan, L. Wang, Y. Tian, X. Xia, Z. Chen, *Nature* **540** (2016) 466–469.
39. I. Forné, J. Ludwigsen, A. Imhof, P. B. Becker, F. Mueller-Planitz, *Mol. Cell Proteomics.* **11** (2012)
40. J. Ludwigsen, S. Pfennig, A. K. Singh, C. Schindler, N. Harrer, I. Forné, M. Zacharias, F. Mueller-Planitz, *eLife* **6** (2017)
41. J. M. Berg, J. L. Tymoczko, L. Stryer, *Biochemistry Lehninger principles of biochemistry*, W. H. Freeman, New York, 2012, p35
42. <http://slideplayer.com/slide/8041509/> (5th September 2017)
43. <https://www.thermofisher.com/de/de/home/references/molecular-probes-the-handbook/thiol-reactive-probes.html> (1st September 2017)
44. https://employees.csbsju.edu/hjakubowski/classes/ch331/protstructure/PS_2A6_Rx_Cys.html (2nd September 2017)

45. M. Berlich, S. Menge, I. Bruns, J. Schmidt, B. Schneider, G. J. Krauss, *Analyst* **127** (2002) 333-336
46. N. Catsimpoolas, J.L. Wood, *J. Biol. Chem.* **241** (1966) 1790-1796.
47. G. R. Jacobsen, M. H. Schaffer, G. R. Stark, T. C. Vanaman, *J. Biol. Chem.* **248** (1973) 6583-6591.
48. Y. Degani, A. Patchornick, 1974. *Biochemistry* **13** (1974) 1-11.
49. N. C. Price, *Biochem. J.* **159** (1976) 177-180
50. H. S. Lu, R. W. Gracy, *Arch. Biochem. Biophys.* **212** (1981) 347-359.
51. N. D. Denslow, H. P. Nguyen, in (D.R. Marshak, ed.) *Techniques in Protein Chemistry*, Vol. 8, Academic Press, San Diego 1996, pp. 241-248.
52. R. Bernstein, K. L. Schmidt, P. B. Harbury, S. Marquseeb, *Proc. Natl. Acad. Sci. U. S. A.* **108** (2011) 10532–10537.
53. P. J. Britto, L. Knipling, J. Wolff, *J. Biol. Chem.* **277** (2002) 29018-29027.
54. M. Bogdanov, W. Zhang, J. Xie, W. Dowhan, *Methods.* **36** (2005) 148-171.
55. E. T. Chouchani, A. M. James, I. M. Fearnley, K. S. Lilley, M. P. Murphy, *Curr Opin Chem Biol.* **15** (2011) 120–128.
56. A. R. Chaudhuri, I. A. Khan, R. F. Ludueña, *Biochemistry.* **40** (2001) 8834–8841.
57. R. Daniel, E. Caminade, A. Martel, F. Le Goffic, D. Canosa, M. Carrascal, J. Abian, *J. Biol. Chem.* **272** (1997) 26934-26939.
58. A. S. Burguete, P. B. Harbury, S. R. Pfeffer, *Nat. Methods* **1** (2004) 55-60.
59. http://web.expasy.org/peptide_cutter/ (1st September 2017)

§ 8. CURRICULUM VITAE

Personal information

First and last name: Petra Vizjak

Date of birth: 01/02/1991

Place of birth: Varaždin

Education

1997–2005	Osnovna škola "Podrute", područna škola Završje
2005–2009	Prva gimnazija Varaždin, Varaždin Prirodoslovno-matematički smjer
2009–2012	univ. bacc. chem. University of Zagreb, Zagreb
2012-2015	mag. biol. mol. University of Zagreb, Zagreb
05-09/2014	Erasmus placement Ludwig-Maximilians Universität, München
2013-2014	Erasmus exchange Technische Universität Dresden, Dresden

Honours and awards

- 2014 - First prize, Pliva Case Study Competition
- 2013 - Special rector's award for project Magic in Science
- 2009 - Scholarship from Grad Zagreb
- 2009 - award for the best student of generation from Prva gimnazija Varaždin
- 2009 - International Chemistry Olympiad, silver medal, Cambridge, UK
- 2008 - International Chemistry Olympiad, Budapest, Hungary

Participation in science popularization

2012-2014 Night of biology and Open doors of Chemistry department

Participation in scientific conferences

1. P. Vizjak, N. Hepp, F. Müller-Planitz, *Remodeling of a folded nucleosome array by ATPase ISWI*, EMBO Conference: The nucleosome: From Atoms to Genomes, Heidelberg, 2017, Abstract book pp. 125.

Publication

1. E. Rücker-Braun, C. S. Link, M. Schmiedgen, A. Tunger, P. Vizjak, R. Teipel, R. Wehner, D. Kühn, Y. F. Fuchs, U. Oelschlägel, L. Germeroth, M. Schmitz, M. Bornhäuser, J. Schetelig, F. Heidenreich, *Exp. Hematol.* **44** (2016) 1024-1033.